Hydrogeological modelling for the watershed management of the Mar Menor coastal lagoon (Spain)

Andrés Alcolea[1], Sergio Contreras[2], Johannes E. Hunink[2],

José Luis García-Aróstegui[3,4], Joaquín Jiménez-Martínez[5,6*]

[1]*HydroGeoModels AG, Tösstalstrasse 23, 8400 Winterthur, Switzerland.*

[2]*FutureWater, Calle San Diego 17, 30202 Cartagena, Spain.*

[3]*Geological Survey of Spain, Murcia Office, Avda. Miguel de Cervantes 45, 5A, 30009 Murcia, Spain.*

[4]*University of Murcia, Institute for Water and Environment, Campus de Espinardo, 30010 Murcia, Spain.*

[5]*Department of Water Resources and Drinking Water, EAWAG, 8600 Dübendorf, Switzerland.*

[6]*Department of Civil, Environmental and Geomatic Engineering, ETH Zürich, 8093 Zürich, Switzerland.*

* Corresponding author: joaquin.jimenez@eawag.ch; jjimenez@ethz.ch

ABSTRACT

The Mar Menor is the largest lagoon along the Spanish Mediterranean coast. It suffers from eutrophication and algal blooms associated with intensive agricultural activities and urban pressure in the surrounding Campo de Cartagena plain. A balanced discharge of groundwater, carrier of algal nutrients such as nitrate, is essential to ensure the integrity of the coastal lagoon and the availability of groundwater resources inland. We here present a 3D hydrogeological model of the unconfined Quaternary aquifer that discharges into the lagoon. The model couples both surface water balance and groundwater dynamics and has been calibrated

25 to available data in the period 2000–2016. The calibrated model allows understanding of the current state

26 of the aquifer and its link to the lagoon. The potential discharge has been quantified in both space and time

27 and falls between 69.5 and 84.9 hm³/yr during dry and wet periods, respectively (with values of nitrate

28 discharge of 11.4–11.8 Mkg/yr in the absence of aquifer sink terms, e.g., leakage to deeper aquifers and

29 pumping from groundwater wells). The predictive capabilities of the calibrated model can be used to test

30 the impact of different integrated management scenarios on the surface-groundwater dynamics of the

31 catchment. Three plausible management scenarios are proposed that include localized and distributed

32 groundwater pumping (drains and groundwater wells, respectively). Results show the effectiveness of the

33 scenarios in reducing the groundwater and nitrate discharge into the lagoon. The disadvantages of the

34 proposed scenarios, including potential seawater intrusion, need to be balanced with their relative merits

35 for the sustainable development of the region and the survival of the Mar Menor ecosystem. The modelling

36 approach proposed provides a valuable tool for the integrated and holistic management of the Campo de

37 Cartagena-Mar Menor catchment and should be of great interest to similar hydrological systems with high

38 ecological value.

39

40 **Keywords**: 3D hydrogeological modelling, integrated watershed management, eutrophication, Campo de

41 Cartagena, Mar Menor coastal lagoon.

42

43

44 **1. Introduction**

45 Coastal lagoons are shallow coastal water bodies, separated from the ocean by sedimentary or anthropic

46 barriers, but connected to it (at least temporarily) by one or several inlets (Kjerfve, 1994, Duck and da Silva,

47 2012). They are important ecosystems (see e.g., Isla, 1995) and sustain numerous economic activities like

48 fishery and tourism. However, their location, generally near densely populated areas, and the often poor

49 water renewal make coastal lagoons highly vulnerable. Amongst other threats, eutrophication has been

50 identified as a major concern over the last decades (Le Moal et al., 2019). Eutrophication of coastal lagoons

51 is a serious problem worldwide (see e.g., the cases of Ria Formosa, Portugal, Newton et al., 2003; Maryland,

52 US, Boynton et al., 1996; Sacca de Goro, Italy, Naidi and Viaroli, 2002; Lake Shinji, Japan, Nakamura and

53 Kerciku, 2000; Lagune de Thau, France, Mesnage and Picot, 1995; Rhode Island, US, Lee and Olsen,

54 1985). The input of nutrients to coastal lagoons contributes dramatically to algal blooms (Breininger et al.,

55 2017) that can reach levels of toxicity to wildlife and humans. Thus, eutrophication also causes negative

56 impacts on tourism and, correspondingly, on the economy (McCrakin et al., 2017). Anthropogenic activities

57 are the main sources of nutrients and are of two kinds, point source and diffuse. The point source

58 contribution of the surrounding hydrological surface network to eutrophication (e.g., after spills) has

59 received attention by the authorities and in the literature (e.g., Arellano-Aguilar et al., 2017; Velasco et al.,

60 2005). However, the diffuse contribution of submarine discharge of groundwater is usually ignored due to

61 the opacity of this process (Robinson et al., 2017).

62

63 Unconfined coastal aquifers play a key role in the eutrophication of coastal lagoons because they usually

64 control the submarine discharge of groundwater with transported chemicals (Dimova et al., 2017; Menció

65 et al., 2017). Thus, understanding the interactions between aquifer and lagoon in both seaward and landward

66 directions is critical for the sustainable management of water resources in coastal areas. For example, the

67 intensive pumping of groundwater may result in seawater intrusion, whereas the practice of intensive

68 agriculture may lead to the discharge of groundwater with a high chemical load (see e.g., Rodellas et al.,

69 2015). In regions where agriculture involves nitrogen (and to a lesser extent) phosphorous-based fertilizers,

70 unconfined coastal aquifers behave as buffers that introduce a time lag between the leaching of fertilizers

71 (Ascott et al., 2017) and their potential discharge into the lagoon (Gilmore et al., 2016; Vero et al., 2018).

72 Therefore, an accurate evaluation of the budget of fertilizers in groundwater is essential to forecast the

73 discharge of nutrients into the lagoon (and in general into other water bodies). Integrated numerical models

74 of surface/groundwater flow and contaminant transport are useful to that end. Unfortunately, the main

75 inputs to such models (e.g., the geometry of the system and its physical properties, forcing terms like

76 pumping rates) are highly uncertain and long-term monitoring of the aquifer (which is rarely available) is

77 required to build representative (in the sense of calibrated) models with predictive capabilities for the

78 integrated and sustainable management of surface water and groundwater resources.

79

80 The modelling of unconfined aquifers connected to coastal lagoons with poor water renewal (e.g., not

81 affected by tides) is a difficult task. At the watershed scale, the main forcing term inland, i.e., aquifer

82 recharge, usually exhibits wide spatio-temporal variability (Santos et al., 2012; Han et al., 2017; Rodríguez-

83 Gallego et al., 2017). At a smaller scale, the modelling of groundwater dynamics near to the coast is further

84 complicated by (1) aquifer heterogeneity, (2) evaporation of groundwater at shallow depths and of surface

85 water in wetlands, e.g., saltmarshes, and (3) variable-density effects (Werner et al., 2013). The interplay

86 between these factors is highly non-linear. For example, evaporation increases groundwater salinity, that

87 leads to salt accumulation (Shokri and Or, 2011) and to local density-driven effects, also aggravated by

88 aquifer heterogeneity, which controls the spatial distribution of submarine discharge. The experimental

89 evaluation of the separate contribution of these effects is difficult, even hardly possible. Numerical

90 modelling is often used to characterize the behaviour of such complex hydrological systems, regardless of

91 their scale. In addition, numerical models are useful to integrate all available information, and are therefore

92 well-suited and objective tools for decision-making, management of water resources and the planning of

93 future monitoring surveys (Candela et al., 2013).

94

95 Here, we present a numerical model to quantify the discharge of groundwater and nitrogen-based fertilizers

96 from an unconfined Quaternary aquifer into the Mar Menor coastal lagoon (SE Spain). The Mar Menor

97 lagoon and its watershed, the Campo de Cartagena plain, are one of the most representative examples of

98 highly anthropized area in the Mediterranean coast. The Mar Menor (literally translated as "The Small

99 Sea"), is actually the largest lagoon along the Spanish Mediterranean coastline and has been catalogued as

100 a protected area under several lists: (1) the Ramsar Convention of Wetlands (https://rsis.ramsar.org/ris/706),

101 (2) Special Protected Areas of Mediterranean Interest (http://www.rac-spa.org/spami), (3) the EU 79/409

102 Birds Directive, and (4) the Nature 2000 Network as a Site of Community Importance

103   (http://www.mpatlas.org/mpa/sites/12699/). The main land use in the surrounding area includes rainfed and

104   irrigated intensive agriculture that, along with high urban pressure, are the main contributors to the

105   eutrophication of the Mar Menor lagoon, which has already suffered recent episodes of algal bloom.

106   Groundwater discharge has recently been demonstrated to be the main source of nutrient-enriched water

107   (Jiménez-Martínez et al., 2016). Groundwater discharge is heterogeneous both in space and time, and in

108   quality and quantity due to the seasonality of crops and the unevenly distributed rainfall events (i.e., mainly

109   short rainstorms). Therefore, to better understand the link between discharge and eutrophication, it is

110   necessary to use a dynamic process-based numerical model that integrates both surface water and

111   groundwater dynamics. We have developed a novel 3D variable-density hydrogeological model to improve

112   the current understanding of the impact of (1) the chronic environmental stressors (i.e., increase in aquifer

113   recharge and the load of agrochemicals resulting from an increase in intensive agriculture in the area) and

114   (2) the anthropogenic perturbations (e.g., shallow drains parallel to the coastline) on discharge into the

115   coastal lagoon. The model is capable of reconstructing the discharge of groundwater over the last two

116   decades (October 2000–December 2016) and provides a reliable characterization of the current state of the

117   aquifer–lagoon system. We also use the model as a predictive tool to analyse the relative merits and

118   drawbacks of so-called mitigation measures, aimed at reducing the discharge of nutrients into the lagoon to

119   prevent a progressive decline and eventual collapse of the ecosystem. In particular, two so-called localized

120   scenarios involving current and newly designed drains to intercept more discharge, and a distributed

121   groundwater-pumping scenario were devised in close consultation with local authorities and stakeholders.

122

123   This paper is organized as follows. First, the study area, the model and the suggested scenarios are described

124   in detail. Second, results are presented and discussed. Finally, the paper ends with some conclusions about

125   the use of modelling techniques for the integrated management of surface water and groundwater resources

126   in coastal areas, and for designing mitigation measures to protect endangered ecosystems in coastal lagoons

127   under high anthropic pressure.

128

2. Methodology

2.1. Study area

The catchment of the Mar Menor coastal lagoon is the Campo de Cartagena plain (SE Spain), with a surface area of 1316 km^2 (Figure 1a). The plain has a gentle slope towards the east (1%) and is surrounded by low mountain ranges except in the east, where the lagoon is located. This region has a semi-arid climate with a mean annual temperature of 18 ºC, an average annual precipitation of 300 mm, and a potential evapotranspiration of 1275 mm/yr (Sanchez et al., 1989). Rainfall is highly variable both in space and time, and is unevenly distributed into a few intensive events, mainly during spring and autumn. Agriculture is the main land use, both rainfed (including almond, winter cereals and olive, covering 6% of the area) and intensively irrigated (including horticultural crops and citrus trees, 31% of the area). Drip irrigation is the most extended practice (90%) due to water scarcity (Alcon et al., 2011). Historically, the water demand for irrigation has been covered by the Tajo-Segura Water Transfer (T-S WT, established in 1979, <1/3 of the demand) and groundwater pumping (<2/3). However, the unmet water demand for irrigation and the recent development of tourism in the area has led to the construction of seawater desalinization plants. The high operational costs of such plants has limited their use for irrigation (Lapuente, 2012; Martin-Gorriz et al., 2014), forcing farmers to install small, privately owned, desalinization equipment to reduce the salinity of the low quality pumped groundwater (Aparicio et al., 2017).

The surface hydrology network draining into the Mar Menor coastal lagoon consists of non-permanent watercourses flowing only during (and shortly after) episodes of intense rain. Since the implementation of T-S WT, groundwater levels have risen as a consequence of the irrigation return flows. This has made some watercourses behave partially (close to the mouth) and temporally like small rivers (García-Pintado et al., 2007) since the 1920s. The groundwater resource is provided by a sedimentary multi-layered system with geological ages ranging from Neogene (Tortonian) to Quaternary. Overall, the hydrogeological system is constituted by three deep confined aquifers of Tortonian, Messinian and Pliocene ages (from bottom to

154 top), and a Quaternary unconfined shallow aquifer (Jiménez-Martínez et al., 2012). The latter discharges

155 into the Mar Menor lagoon and is the object of this study. The Quaternary aquifer, highly polluted by

156 agrochemicals due to irrigation return flows, covers almost the entire Campo de Cartagena plain (Figure

157 1a). The high density of abandoned, poorly constructed (in the sense of leaky) deep wells induces cross-

158 formational groundwater flows and contamination of the confined deeper aquifers at the local scale

159 (Jiménez-Martínez et al., 2011; Baudron et al., 2013). At the regional scale, the spatio-temporal

160 distributions of groundwater levels in the shallow unconfined and in the deeper confined aquifers are

161 independent (García-Aróstegui et al., 2017).

162

163 The Mar Menor lagoon (Figure 1b) has a surface of 135 km^2 and a volume of 593 hm^3, with mean depth

164 4.5 m and maximum depth <6.5 m. The lagoon is one of the largest in the Mediterranean basin (Perez-

165 Ruzafa et al., 2011, 2013) and the largest along the Spanish Mediterranean coast. It is separated from the

166 open sea by a 22-km-long sand bar (La Manga), although one natural inlet and two artificial channels allow

167 some water renewal (water velocity in the lagoon is lower than 0.03 m/s; García-Oliva et al., 2018). This

168 valuable ecosystem has been degraded over the last decades, with flora and fauna as bio-indicators of the

169 trophic changes (Perez-Ruzafa et al., 2007). Anthropogenic pressure on the lagoon is related to: (1) the

170 opening and dredging of artificial inlets in the sandbar, which have induced changes in the hydrodynamics

171 and water balance of the lagoon (so-called "Mediterraneanisation", Perez-Ruzafa et al., 2009); (2) the acid

172 drainage of heavy metals from an abandoned mining area (Cartagena-La Unión mining district in Figure

173 1a; Jimenez-Carceles and Alvarez-Rogel, 2008); (3) the discharge of nutrients from both the surface water

174 network and groundwater (average nitrate concentration in the lagoon <1 mg/L, but with peaks up to 3.5

175 mg/L, Baudron et al., 2015; Velasco et al., 2005), a by-product of the intensive agricultural activity in spite

176 of the retention and degradation taking place in the saltmarshes surrounding the lagoon (Tercero et al.,

177 2017); and (4) the emerging input of organic contaminants of concern from agricultural activities and urban

178 water spills (Moreno-Gonzalez et al., 2015; Traverso-Soto et al., 2015). Past and current economic activities

179 have converted the Mar Menor lagoon, markedly oligotrophic in its natural regime, into a highly

180 eutrophicated ecosystem (Perez-Ruzafa et al., 2009), collaterally damaging other activities such as fishery

181 and tourism (Marcos et al., 2015). For a detailed review of the environmental stressors and impacts on the

182 Mar Menor lagoon, the reader is referred to Jiménez-Martínez et al. (2016).

183

2.2. Model description

185 A three-dimensional (3D) hydrogeological model was built that couples a surface water balance model with

186 a groundwater model. Compared to 2D models, 3D models require significantly more resources in terms of

187 CPU and data for their parameterization, calibration and validation. In exchange, 3D models allow density-

188 driven effects to be addressed, in this case at the interface between the unconfined aquifer and the lagoon.

189 The surface water balance and its main components were quantified with the open-source SPHY (Spatial

190 Processes in Hydrology) bucket-type modelling code (Terink et al., 2015), previously adapted for the study

191 region by Contreras et al. (2014, 2017). In this study, SPHY computes the main water balance components

192 and soil moisture dynamics at discrete soil layers and on a daily basis. The water balance at the root zone

193 is primarily controlled by soil moisture (i.e., the state variable), the inflows from precipitation and the main

194 water losses due to interception and actual evapotranspiration. The latter are driven by vegetation (satellite-

195 based vegetation greenness and fractional vegetation cover), root depth, water storage and soil texture.

196 Lateral fluxes in the vadose zone are neglected. This assumption is acceptable due to the smooth topography

197 in the studied area (i.e., bout 90% with slopes <1%). As such, vadose flows are mainly attributed to capillary

198 forces, whose effect is minor and local. Therefore, the non-evapotranspirated fraction of precipitation that

199 exceeds the storage capacity of the soil is computed as potential recharge to the shallow aquifer.

200

201 The main inputs to the SPHY model are both static and dynamic. The static inputs are terrain slope (derived

202 from a Digital Elevation Model) and the main hydraulic properties of the soil, which can be derived from

203 soil textural maps and pedotransfer functions (Wösten et al., 2001). The main dynamic inputs are derived

8

204   from climate data (precipitation and Penman-Monteith reference evapotranspiration) and satellite-based

205   vegetation data (Normalized Difference Vegetation Index -NDVI-, used as a surrogate of the vegetation

206   growth phenology and productivity). The main outputs of SPHY are evapotranspiration losses and aquifer

207   recharge, which is used as input to the 3D variable-density groundwater model. Groundwater flow is solved

208   with the open-source finite elements code SUTRA (Saturated-Unsaturated TRAnsport, Voss and Provost,

209   2010). Aquifer properties (hydraulic conductivity and storativity) are heterogeneous and calibrated using

210   the Regularized Pilot Points Method (Alcolea et al., 2006), as implemented in the generic calibration

211   software PEST (Doherty, 2016).

212

213   2.3. Model setup

214   The surface water model encompasses a surface area of 2235 km^2 divided into 35,760 cells of 250 x 250 m

215   (a control volume of 62,500 m^2, the third dimension being the root depth). It is larger than the groundwater

216   model, which spans the Quaternary aquifer only, to account for surface runoff to other surrounding

217   watersheds. The meteorological data sets (precipitation and reference evapotranspiration) required to

218   simulate the period October 2000–December 2016 were obtained from the SIAM network

219   (http://siam.imida.es/), which includes 12 stations for the modelled area and 4 out of it (also used for the

220   calculation of isohyets; Figure 2a). Station-based measurements were spatially interpolated using a spline

221   method. A land-cover map (project SIOSE2005, http://www.siose.es/) was used as auxiliary data to identify

222   natural or rainfed areas and the main irrigated cropping systems (dominated by citrus and seasonal crop

223   systems). Evapotranspiration and crop coefficients were obtained from the NDVI (extracted from the

224   MODIS MOD13Q1 product – collection 6, tile h17v05; average values over 16 days; Villalobos et al.,

225   2006). Soil properties, including soil (root) depth, field capacity and wilting point are heterogeneous in the

226   surface water model. In particular, the spatial distributions of field capacity (3 atm on average) and wilting

227   point (15 atm on average) were computed using pedotransfer functions accounting for both soil texture and

9

228 organic matter contents identified in the LUCDEME project (Perez-Cutillas, 2013). More details on the

229 procedure can be found in Contreras et al., 2014, 2017).

230

231 The geometric definition of the Campo de Cartagena Quaternary aquifer (1119 km^2), and its continuity

232 below the Mar Menor lagoon (135 km^2), builds upon the 3D geological model proposed by Jiménez-

233 Martínez et al. (2012), in which a spatial resolution based on 500 × 500 m cells was adopted. The Quaternary

234 aquifer is made of sand, silt, clay and conglomerates and has an average thickness of 50 m, increasing from

235 west to east and reaching ~150 m near the lagoon. The aquitard below is made of very low conductive marls

236 and evaporates of the Pliocene with an average thickness of 60 m. This unit and the deeper confined aquifers

237 are not modelled, due to the negligible natural fluxes (i.e., those caused by raw vertical hydraulic gradient)

238 from the top Quaternary to the subjacent Pliocene and Messinian aquifers at the regional scale (Jiménez-

239 Martínez et al., 2011; García-Aróstegui et al., 2017).

240

241 The horizontal discretization of the 3D model was carried out with finite elements of irregular size, with

242 local refinements near zones with high topographic gradient (i.e., honouring the surface hydrology

243 network), along the coastline and near the current network of drains (Figure 2b). The vertical discretization

244 consists of 10 layers of elements, whose vertical size depends on aquifer thickness. Overall, the 3D mesh

245 contains 8 million hexahedral and prismatic finite elements (Figure 2c). Initial conditions are, as is often

246 the case in practice, highly uncertain. In order to minimize their impact, we model a long time period of 16

247 years (October 2000 to December 2016) that covers a wide range of hydrometeorological conditions.

248 Particularly relevant to this study are the identified hydrometeorological average (April 2002–March 2004),

249 wet (September 2008–August 2010) and dry periods (September 2013–August 2015). The impact of the

250 initial conditions on model results was evaluated by simulating the 16-year period using different starting

251 situations, showing that the results after December 2000 are independent of the chosen initial condition.

252 The model boundary conditions of the groundwater model are as follows:

253 (1) The western boundary coincides with a surface water divide. It is assumed that the underground water

254   divide approximately follows that contour and, correspondingly, an impervious boundary is assigned.

255   The impact of this assumption on the discharge of groundwater is negligible due to the large extent of

256   the model in the direction west to east (~43 km).

257 (2) The northern and southern boundaries of the model are the limits of the Quaternary aquifer. An

258   impervious boundary condition is assigned. Thus, it is assumed that the lateral contributions from or to

259   other aquifers (especially along the northern boundary) are negligible compared to recharge and

260   discharge.

261 (3) The eastern boundary is the lagoon, the volume of which is explicitly modelled. Nodes defining the

262   lagoon are attributed with a constant head boundary condition (0 m of equivalent fresh water level) and

263   a relative salt concentration of 37 kg/m^3 (0 kg/m^3 for nodes inland). Tides are not considered in the

264   model, since the lagoon regime is microtidal, with tidal range smaller than 0.6 m (maximum

265   astronomical tidal range in open sea in the vicinity, Sánchez-Badorrey and Jalón-Rojas, 2015). Such

266   fluctuations may cause local spatiotemporal perturbations of the hydraulic regime near the coastline.

267   However, their impact on groundwater levels is dampened by the temporal discretization of the model

268   (i.e., day-long intervals).

269 (4) The existing intra-basin water transfer Tajo-Segura and Taibilla channels, for agricultural and drinking

270   water supply purposes, respectively, are relatively modern (1979 and 1946, respectively) and under

271   continuous inspection. Thus, water losses from these infrastructures are negligible and ignored as water

272   sources for the aquifer.

273 (5) The six existing drains (Figure 2a) with corresponding temporal series of pumping rates are modelled

274   individually by means of distributed prescribed flow boundary conditions. The overall pumping is, on

275   average, <0.7 hm^3/yr. The existing drains perform as constant head boundaries. To mimic that effect,

276   their geometry is explicitly included in the model. Similarly, their hydraulic parameters are estimated

277   separately.

278   (6) Active and abandoned pumping wells cannot be explicitly modelled due to lack of information (i.e.,

279   unknown location or history of pumped volumes). Notably, ~500 deep abandoned and poorly

280   constructed wells (>150 m depth) are distributed over the model domain, with higher density near the

281   coastline (Jiménez-Martínez et al., 2011). Such potentially leaky wells communicate the shallow

282   aquifer with the deep aquifers. The total volume of water transferred by leaky wells or pumped from

283   active groundwater wells was estimated by hydrochemical balance to be approximately 30–40% of the

284   overall recharge (Jiménez-Martínez et al., 2011). This large volume of groundwater does not reach the

285   lagoon and therefore, has a major impact on the volume of discharge, on the storativity of the system

286   or on both. Unfortunately, these "losses" (in the sense of aquifer sinks) cannot be accounted for directly

287   in the model as either point or diffuse sink boundary conditions because neither the coordinates of most

288   abandoned and active boreholes nor their distribution over the aquifer are known. The impact of

289   ignoring these losses on model results is further discussed below.

290

291   As a result of the aforementioned boundary conditions and model simplifications, the groundwater model

292   is a bucket model, in which the only source term is the recharge calculated by SPHY and the sink terms are

293   the discharge to the lagoon and the pumping from existing drains. Since losses caused by localized pumping

294   and vertical fluxes along leaky wells cannot be accounted for, model results in terms of discharge of

295   groundwater and nutrients must be taken as upper bounds. The spatial distribution and dose of the chemical

296   load (900–1600 kg/ha/yr, i.e., sum of ammonium nitrate NH_4NO_3, phosphoric acid H_3PO_4, potassium nitrate

297   KNO_3, calcium nitrate $Ca(NO_3)_2$, ammonium phosphate $(NH_4)_3PO_4$, and magnesium nitrate

298    $Mg(NO_3)_2 \cdot 6H_2O$; Jiménez-Martínez et al., 2011) associated with agriculture is known. However, the uptake

299   efficiency of plants, and therefore the rate of percolation of those agrochemicals to the aquifer, is highly

300   uncertain and difficult to model in a simple manner. Concentration data near the coastline are available at

301   six wells (Figure 3). Temporal series display a general increase of nitrate concentration mainly caused by

302   the intensification of agricultural activities (e.g., an increased irrigated surface). The lack of data precludes

303   the explicit modelling of the budget of nutrients. Instead, we focus on possibly the most active contributor

304   to eutrophication, nitrate, and calculate the mass rate discharged into the lagoon by multiplying the

305   discharge of groundwater by the nitrate concentration. To that end, the coastline is divided into six segments

306   that are each attributed the nitrate concentration at the closest monitored well. Thus, it is assumed that

307   nitrate does not degrade along the path from the monitored well to the coastline. This assumption is

308   supported by the oxic character of the unconfined Quaternary aquifer, which precludes the degradation of

309   nitrates (Jiménez-Martínez et al., 2011). In this line of arguments, the denitrification of the upper part of

310   the aquifer underlying coastal wetlands does not play either a major role in nitrate degradation because

311   aquifer thickness is large.

312

313   **2.4. Parameterization and available data**

314   The groundwater flow model is parameterized by two unknown spatial distributions (hydraulic conductivity

315   K [m/d] and specific yield S_y [-], the latter being similar to the aquifer's effective porosity). These

316   parameters can be easily transformed into their 2D counterparts, i.e., transmissivity T [m^2/d] and S [-] by

317   plugging in the aquifer saturated thickness b [m]: $T = Kb$ and $S = S_y + S_s b$, S_S being is the specific storage

318   [m^{-1}]. The low quality and scarcity of parameter data, e.g., arising from the prior analytical interpretation

319   of a few pumping tests (Tragsatec, 2013), precludes the estimation of model parameters on a cell-by-cell

320   basis. In addition, the such fine model discretization would make this computational problem unresolvable

321   in a reasonable amount of time. To overcome this problem, we first assume that model parameters are

322   homogeneous in the vertical direction. This allows us to display the model parameterization in in 2D by

323   plotting hydraulic diffusivity D [m^2/d] = T/S. The hypothesis of vertical homogeneity is supported by the

324   pseudo-homogeneity observed in available stratigraphic sequences from exploration boreholes in the area

325   (Jiménez-Martínez et al., 2012). In contrast, K (especially) and S_y may vary several orders of magnitude

326   over small horizontal distances in Quaternary aquifers. To mimic this pattern, K and S_y are considered

327   heterogeneous and interpolated from values at 72 points distributed over the model domain (so-called pilot

328   points). Artificial drains are assumed to be homogeneous with individual parameterization (overall, 6

329   additional pilot points, one per existing drain). The value of K and S_y at pilot points is estimated via the

330   Regularized Pilot Points Method (RPPM, Alcolea et al., 2006), as implemented in PEST (Doherty, 2016),

331   a general-purpose maximum likelihood estimation software. Parameter calibration requires head data at

332   available boreholes in the area. Unfortunately, heads were measured only after drilling in most cases.

333   Overall, heads were measured more than once at 25 wells only, and long measurement records are available

334   at only 16 of them. Calibration was performed with head data at these 16 boreholes only (overall, 822 head

335   measurements). Remaining measurements (88) were used for model validation. The estimates of model

336   parameters reported in Tragsatec (2013) are included in the model as prior information. The reported

337   storativity values are highly uncertain and attributed a very low weight in the calibration, because the vast

338   majority of hydraulic tests were carried out in a single well (Meier et al., 1999).

339

340   **2.5. Management scenarios**

341   The model setup described so far is used to represent the current state of the system. The calibrated model

342   was then used to simulate three scenarios representing plausible management strategies aimed at reducing

343   the discharge of groundwater and nutrients into the Mar Menor lagoon. These scenarios, which consider

344   different pumping patterns and volumes, were devised in close consultation with the local authorities and

345   are therefore feasible in the near future. They were devised bearing in mind that (1) the expansion of the

346   irrigated area is not allowed by law, and (2) the overall goal is to reduce the release of agrochemical by-

347   products into the coastal lagoon. The model forecasts must be considered from a qualitative point of view

348   only, since the socio-economic evolution of the region and the impact of climate change (i.e., variations in

349   recharge) are not considered in the analysis. Nevertheless, the suggested scenarios are well suited to

350   environmental decision-making.

351

352   *Scenario 1.* The first scenario involves the increase of the pumping capacity of the six existing drains that

353   run parallel to the coastline in the southern sector (e.g., by enlarging the current cross section or by replacing

354   clogged filters). The existing drains have been operative since the end of 2008, and have a total length of

355   14.8 km. During the operational period 2008–2016, a mean annual rate of 0.7 hm^3/yr of brackish

356   groundwater was pumped, which means a pumping rate capacity of 0.05 hm^3/km/yr. In this scenario, the

357   current pumping capacity is multiplied by a defined pumping intensification factor α.

358

359   *Scenario 2.* The second scenario involves the existing drains and the construction of a set of new drains

360   with (1) a total length 6.6 km to the north of the Rambla del Albujón (Figure 4) and (2) the design

361   characteristics of the existing drains (i.e., the same pumping rate capacity is assumed). The trace of the

362   proposed new drains accounts for urban areas, topography and current groundwater levels. For instance,

363   the maximum depth of the new drains was set to 6 m, which makes its implementation feasible and not

364   costly. Assuming the same pumping rate capacity as the existing drains, this scenario accounts for a total

365   pumping of 1 hm^3/yr. As in scenario 1, a pumping intensification factor α is used to evaluate the impact of

366   a more intense pumping strategy on the discharge of groundwater and nutrients into the lagoon.

367

368   Scenarios 1 and 2 are described here as *localized scenarios* because pumping takes place along localized

369   linear infrastructures. In both cases, the high salt and nitrate content of the pumped groundwater must be

370   removed prior to its use for irrigation purposes (as it is done nowadays in the southern sector). This would

371   include the construction of new treatment facilities and/or the conduction of the pumped water to the

372   existing ones. The management of sub-products such as rejected brackish water would also need to be

373   included in an integral management plan, which is far beyond the scope of this paper.

374

375   *Scenario 3.* The third scenario, described here as a *distributed scenario*, envisions the pumping of

376   groundwater at the many wells scattered over the irrigated area, which are coupled with private

377   desalinization plants. The pumping from the current drains is included, but not the construction of the new

378   drains suggested in scenario 2. The water demand for agricultural purposes in the T-S WT irrigation sectors

379   (shaded area in Figure 4) is on average 76 hm^3/yr and is mostly supplied by the T-S WT (on average 61

380   hm^3/yr, but highly variable with a maximum value of 132 hm^3/yr in 2014; Jiménez-Martínez et al., 2016).

381   The remaining water demand is covered by groundwater pumped from the deep confined aquifers (on

382   average 15 hm^3/yr), whose quality for irrigation purposes is better than that pumped from the Quaternary

383   shallow aquifer. The third scenario suggests pumping from the shallow aquifer instead, which would reduce

384   the discharge of polluted groundwater into the lagoon and, in addition, preserve the confined aquifers. The

385   spatial pumping pattern assumed in this scenario follows that of groundwater use per irrigation sector

386   described in Hunink et al. (2015). As for the *localized scenarios*, the necessary additional infrastructure for

387   the desalination/denitrification of brackish water is not considered here.

388

389   **3. Results**

390   **3.1. Model performance and parameterization**

391   The performance of the calibrated model is evaluated both in terms of goodness of fit to available hydraulic

392   head measurements and plausibility of the calibrated model parameters. Figure 5 shows a scatter plot of the

393   measured and calculated heads after the calibration and validation exercises, and the histogram of residuals

394   (calculated minus measured value) after calibration. The Root Mean Square Error (RMSE) is 1.3 and 4.3

395   m for calibration and validation, respectively, while the corresponding Maximum Absolute Errors (MAE)

396   are 4.3 and 14.6 m. The model tends to slightly overestimate heads at some points (Figure 5a), which leads

397   to a right tail in the residuals (Figure 5b). This was expected because head measurements at a few points

398   were collected during pumping. Unfortunately, the corresponding dates of pumping are not reported and

399   those measurements cannot be filtered. An additional contribution to the positive misfit is the proximity of

400   some monitored wells to active pumping wells, which cause a drawdown that is captured in the

401   measurements but not by the model (i.e., because the location of pumping wells and/or the pumping rates

402   are unknown). Nonetheless, both calibration and validation fits are acceptable, with mean residuals of 0.27

403   and 1.29 m respectively. Fits to available data at selected observation points are presented in section 3.2.

404

405   Model parameters K and S_y are presented in terms of hydraulic diffusivity in Figure 6a. Note that hydraulic

406   parameters of existing drains were estimated separately and are not reported in Figure 6a because the mean

407   estimated diffusivity at drains is ~500 m^2/d, which would distort the colour bar. This very high value stems

408   from their high hydraulic conductivity and very low storativity. Figure 6b shows the posterior parameter

409   uncertainty, as measured by the posterior standard deviation of model parameters σ. The 95% confidence

410   interval of a given model parameter p is calculated on a log scale as $log_{10}p \pm 2\sigma$. Thus, small values of σ

411   are translated into low uncertainty of the estimated parameters. The largest σ values are found near the La

412   Unión mining district (in the south), where no head data are available, and near the mouth of the Rambla

413   del Albujón (on the western-most point on the lagoon). The latter received the rejected by-product of

414   desalinization plants, thus behaving sporadically like a river that infiltrates brackish water. The leakage of

415   the surface drainage network is not considered in the model because of lack of information. However,

416   available head measurements in the vicinity are affected by the river–groundwater seepage connection.

417   Thus, it is not unexpected that the calibration process, in an attempt to fit head data that cannot be fitted

418   with current boundary conditions, suffers from some instability that inflates the posterior standard

419   deviation. Overall, posterior standard deviations are small and far below 1. This means that the lower and

420   upper bounds of the confidence interval of an estimated parameter are always within the same order of

421   magnitude.

422

3.2. Evolution towards the current state

424   The calibrated model allows evaluation of the current state of the aquifer, the different components of the

425   water balance and their relationships. Recharge and discharge are the main mechanisms driving the

426   hydrodynamic system and are modelled explicitly. As described above, vertical losses from the shallow to

427   deeper aquifers and pumping wells are not modelled due to lack of information. Thus, the discharge rates

428   of groundwater and nitrate presented in this section are upper bounds and correspond to the most pessimistic

429   situation from an ecological point of view.

430

431   Recharge varies greatly from one day to the next and also exhibits marked seasonal and yearly trends, which

432   cause fluctuations in discharge, partly dampened by the aquifer. Although technologically sounding and

433   with high irrigation efficiency, agricultural practices cause sometimes peaks in the temporal distribution of

434   recharge. Such peaks are favoured by (1) the shallow topographic gradient towards the east, which hinders

435   surface run-off, and (2) the combination of the rainfall characteristic of semi-arid regions (i.e., unevenly

436   distributed into a few intensive events highly variable in space and time) and the high water content of the

437   soil caused by the permanent agricultural activity, which increases relative hydraulic conductivity, thus

438   favouring recharge (Jiménez-Martínez, 2010).

439

440   Figure 7a shows the estimated mean annual recharge for the studied period 2000–2016. The mean annual

441   recharge is ~73 mm/yr, but higher values of ~300 mm/yr are found in the southeast irrigated area. These

442   values are consistent with the results of in situ studies that took into account the most representative crops

443   and agricultural practices in the region, i.e., rotation of lettuce and melon, artichoke, and citrus, all of them

444   under drip irrigation (Jiménez-Martínez et al., 2010). Figure 7b shows the monthly averaged water mass

445   balance components for the study period (2000-2016), i.e., precipitation and irrigation as inflows, and actual

446   evapotranspiration, surface runoff, interception and recharge as outflows. Figure 8 shows the contours of

447   hydraulic heads calculated with the calibrated model for the considered average hydrometeorological period

448   April 2002–March 2004. The hydraulic gradient increases from west to east. The increase is highly non-

449   linear and very rapid in the vicinity of the coastline. The overall distribution of hydraulic heads does not

450   vary greatly in time. In fact, the head fluctuation during dry and wet periods (around mean values during

451   the average period) is only -0.5 and 2 m, respectively. The temporal evolution of hydraulic heads at selected

452   points is also shown in Figure 8. Several observations are apparent in these plots: (1) a decreasing trend of

453   heads with time, directly related to the proliferation of small private desalinization plants (i.e., a situation

454   similar to that suggested by the distributed scenario), (2) a partial recovery of groundwater levels during

455   the wet period (September 2008–August 2010), and (3) the strong reaction of the aquifer to episodic peaks

456   in recharge. Finally, the maximum penetration of the saltwater wedge (i.e., the toe, green line in Figure 8)

457   for the average period is <330 m. The penetration of the toe during dry and wet periods is very similar

458   (shifts of a few tens of meters with respect to the toe during the average period) and the fluctuation is not

459   reported in Figure 8.

460

461   The calibrated model was used to quantify the spatio-temporal distribution of groundwater and nitrate

462   discharge into the lagoon (Figure 9). The perimeter of the lagoon was divided into 15 segments of length

463   ~2 km, taking as starting point the mouth of the Rambla del Albujón. For each segment, the fluxes of

464   groundwater at the corresponding nodes are integrated daily, which yields the total daily discharge of

465   groundwater along the segment. The discharge of nitrates is calculated by multiplying the daily discharge

466   of groundwater by nitrate concentration at the closest monitored borehole in Figure 3. The discharge occurs

467   mainly in the central sector of the lagoon (66–70% of groundwater discharge and 71–75% of nitrate

468   discharge occurs along segments North2 to South2, depending on the hydrometeorological period) and

469   diminishes almost monotonically when moving northwards or southwards. The discharge across segments

470   to the north of the Rambla del Albujón (North1 to North7; 60–62% of total groundwater discharge and 55–

471   58% of total nitrate discharge) is slightly larger than that across southern segments. This is a direct

472   consequence of the pumping from existing drains in the southern part.

473

474   The potential daily discharge of groundwater and nitrate load into the lagoon is shown in Figure 10. These

475   correspond to the sum of the curves presented in Figure 9. Five different periods are apparent:

476   -   From 2000 to 2005, the discharge of groundwater oscillates seasonally around a mean value ~0.19

477   hm^3/d. Strong peaks in the calculated hydrogram are observed in response to peaks in the recharge

478   record corresponding to episodic intense rain events. The discharge of nitrates fluctuates in similar

479   way, around a mean value of ~22,000 kg/d.

480   -   From 2005 to 2009, the discharge of groundwater maintains the same seasonal trend, but the

481   discharge of nitrates increases progressively to ~27,000 kg/d. This is a result of the progressive

482   increase of nitrate concentration in the aquifer (Figure 3).

483   -   From 2009 to 2011, recharge increases substantially (i.e., a wet period), which leads to an increase

484   of the discharge of both groundwater and nitrates, reaching mean stable values of ~0.2 hm^3/d and

485   a plateau ~34,000 kg/d, respectively.

486   -   From 2011 to 2014, recharge and, correspondingly, discharge of groundwater diminish

487   substantially in response to a sequence of mid to dry hydrological years. However, the discharge

488   of nitrates into the lagoon remains stable (and maximum) at ~34,000 kg/d. This is explained by the

489   continued increase of nitrate concentration in the aquifer (Figure 3).

490   -   From 2014 to 2016, the discharge of groundwater continues to diminish, following the trend of the

491   previous period. The discharge of nitrate also diminishes, but more rapidly. This trend is likely a

492   consequence of the introduction of technical improvements in irrigation systems, and represents a

493   hopeful step for the sustainable development of the region and the survival of the Mar Menor

494   ecosystem. The largest rainfall event took place at the end of the simulation period (December

495   2016), which precludes the evaluation of its impact on discharge.

496

497   Table 1 summarizes the components of the water balance during wet, average and dry periods, the mean

498   for the studied period, and the corresponding nitrate loads released into the lagoon. Reported values

499   correspond to averaged model outputs. There are large differences in recharge during the three characteristic

500   periods. However, the maximum discharge of groundwater into the lagoon (i.e., in the sense of potential,

501   ignoring vertical fluxes to deeper aquifers and the pumping from groundwater wells) is relatively constant.

502   The water excess during wet periods is translated into an enhanced capacity of the aquifer that leads to an

503   overall increase of groundwater levels (recall Figure 8). Nonetheless, such variation is small compared to

504   the average volume of groundwater in the aquifer (~2575 hm^3 as evaluated by the model). On average, the

505   maximum discharge of nitrate into the lagoon is relatively similar during the dry and wet periods, but was

506   lower during the earlier average period, as discussed above. We attempted to address the impact of the

507   unconsidered sink terms by subtracting 30% and 40% of the overall recharge (Jiménez-Martínez et al.,

508   2011) from the mean discharge of groundwater (values in italics in Table 1). This reduces the discharge of

509   groundwater by a factor 1.5 to 1.75, assuming that the losses do not have an impact on aquifer storativity.

510   This factor is larger (1.9 to 2.3) considering the discharge of nitrates into the lagoon. The large disparities

511   between maximum (i.e., as calculated) and possible discharge values highlight the need for newly acquired

512   measurements to reduce model uncertainties, mainly caused by lack of information.

513

3.3. Analysis of integrated management scenarios

515   *Localized scenarios.* A simulation of the whole 16 years period was performed. Only the dry and wet

516   hydrometeorological periods were analysed because the existing drains are operative since end of 2008

517   (i.e., not during the average hydrometeorological period). Figure 11a shows the reduction in the discharge

518   of groundwater into the coastal lagoon as a function of pumping rate with either existing or existing together

519   with extended drains. These localized scenarios are not capable of inverting the current flow regime (aquifer

520   to lagoon, positive values of discharge in Figure 11a) during a wet period (blue curves), even if the pumping

521   rate at drains is increased 150-fold with the current or extended drains. The flow regime is inverted during

522   a dry period if the pumping capacity is increased by a factor of 80 (with current drains only) and 60 (current

523   plus extended drains). Figure 11b shows the reduction in discharge in terms of mass flux of nitrate into the

524   lagoon. Both scenarios reduce the discharge of nitrates, particularly the second scenario with extended

525   drains. The reduction in nitrate discharge increases with pumping intensification and is especially large

526   during dry periods. Note that, in this case, the discharge of nitrates is again the maximum possible (i.e., the

527   potential discharge) because sink terms are ignored by the model. As such, the discharge rates presented in

528   Figure 11 must be considered as the most pessimistic situation from an ecological point of view.

529

530   *Distributed scenario.* The distributed pumping of ~15 hm^3/yr from the shallow unconfined Quaternary

531   aquifer (only from the sectors irrigated with water from the T-S WT; shaded area in Figure 4) causes a

532   small reduction in the groundwater discharge into the Mar Menor lagoon during the simulated wet and dry

533   periods (points in Figure 11a). This is equivalent to the reduction caused by a 3–5 times greater pumping

534   rate in the localized scenarios (for dry and wet conditions, respectively). An even greater reduction in the

535   discharge of nitrates is observed (Figure 11b). A maximum reduction of ~2000 kg/d is observed during

536   both dry and wet periods, which corresponds to a high pumping rate (from 10 to 100 times the current one)

537   under the localized scenarios.

538

539   The intersections between the curves in Figure 11a and the horizontal dashed line (0 discharge) represent

540   an old envisaged management strategy known by local stakeholders and policy-makers as "zero spill"

541   (referring to zero spill of nutrients, an unfortunate and misleading term supposed to mean "zero discharge").

542   A zero discharge of groundwater into the lagoon could be achieved during dry periods with pumping

543   intensification factors of 82.5 and 57.5 for scenarios 1 and 2, respectively, and would require even higher

544   values during wet periods. The volumes of pumped groundwater corresponding to such high intensification

545   factors would be 57.8 and 60.4 hm^3/yr for the scenarios 1 (current drains) and 2 (current plus extended

546   drains), respectively. Such volumes are far from being physically plausible. In addition, a null mean

547   discharge (along the whole perimeter of the Mar Menor) does not necessarily imply a null discharge of

548   nutrients. A zero mean discharge of groundwater means that the volume of brackish water pumped from

549   drains is equivalent to the discharge of groundwater along areas not affected by drains, where nitrate

550   discharge would still take place. Moreover, shallow drains have a certain catchment zone and cannot capture

551   the nitrates all along the saturated thickness of the unconfined aquifer (~100 m in the area affected by

552   drains). Thus, nitrate discharge may also take place at the area affected by drains. Consequently, although

553   the drains would capture larger masses of nitrates, a "zero spill" of nutrients into the Mar Menor is, at best,

554 utopic. None the less, the simulation of this "old-fashion" management strategy has been included in Figure

555 11 for completeness only.

556

557

558

559

560

561 **4. Discussion**

562 This section discusses the main strengths and weaknesses of the model and the proposed management

563 scenarios. We start by discussing the main weakness of our work, i.e., that the underlying conceptual model

564 is unquestionably wrong (but forced by the lack of information; Shapiro, 2007). The pumping from

565 groundwater wells and the vertical fluxes from the shallow Quaternary aquifer to the deeper confined

566 aquifers through leaky wells have been ignored because information, hard or soft, is not available to model

567 them explicitly. Instead, we approximated this by applying an overall reduction in the discharge of

568 groundwater into the lagoon (30–40% of the overall recharge, i.e., 26–35 hm^3/yr). We argue that the low

569 quality of groundwater from the Quaternary aquifer (electric conductivity ~5000 μS/cm and >100 mg/L

570 NO$_3^-$) precludes its use for irrigation or any other consumptive use (only 2 hm^3/yr according to ITGE, 1991).

571 This small value partly reduces the consequences of our "forced" hypothesis. In contrast, vertical losses to

572 deeper aquifers may be important. However, we argue that this is not the case in the Campo de Cartagena

573 plain. Distributing 26–35 hm^3/yr uniformly among 500 leaky wells (Jiménez-Martínez et al., 2016) yields

574 an individual loss of 1.7–2.2 L/s. Tragsatec (2013) and Contreras et al. (2017) report reference

575 transmissivity values of up to 1600 m^2/d at zones where aquifer saturated thickness was small (in the range

576 1–10 m, the average being 50 m). As such, even larger transmissivity values can be expected and are

577 actually revealed by the model. Plugging the individual loss rates and this transmissivity value into Thiem's

578 formula (Thiem, 1906) suggests a distributed steady state drawdown ~10–14 cm. This range is comparable

23

579 with the measurement errors (e.g., in the reference elevation of the wells, in the manual collection of head

580 data) and should not alter the hydrodynamic regime in the aquifer, especially because losses are small point

581 sinks in the aquifer that, moreover, are well distributed in space. A second back-of-the-envelope calculation

582 also supports our argument. If a porosity $\phi = 0.15$ is assumed (Contreras et al., 2017), the drop in

583 groundwater levels caused by leaky wells is <15–20 cm (by simply distributing losses uniformly over the

584 1119 km^2 aquifer), which is very low compared to the head fluctuations caused by recharge or by the

585 pumping from existing drains. In fact, the total volume of groundwater stored in the aquifer is ~2575 hm^3

586 (Contreras et al., 2017). Thus, the unconsidered "lost" volume represents 1–1.3% of the total volume of

587 groundwater in the aquifer. In view of these arguments, the available head measurements are unlikely to be

588 perturbed by local losses to underlying aquifers. Thus, the estimated model parameters are unlikely to be

589 affected by the hypothesis of ignoring leaky and active wells.

590

591 The model was calibrated to available measurements in the period October 2000–December 2016. An upper

592 bound of mean groundwater discharge into the lagoon, i.e., in the absence of the aforementioned losses, is

593 78 hm^3/yr. Estimated losses of 26–35 hm^3/yr caused by vertical fluxes and pumping are slightly lower (but

594 still in accordance) with those reported in previous work (38 hm^3/yr by ITGE, 1991; 44.5 hm^3/yr by

595 Domingo-Pinillos et al., 2018 and <46 hm^3/yr by Jiménez-Martínez et al., 2016). The effective discharge

596 of groundwater into the Mar Menor lagoon assuming losses of 26–35 hm^3/yr has been roughly estimated

597 by mass balance in the range 45–53 hm^3/yr (Table 1). This range is quite controversial. For example, ITGE

598 (1991) reported 5 hm^3/yr only, presenting a back-of-the-envelope calculation using a constant head gradient

599 and a homogeneous transmissivity. A similar value (6.2 hm^3/yr) has been recently reported in the

600 Hydrological Plan of the Segura Basin 2015-2021

601 (https://www.chsegura.es/chs/planificacionydma/planificacion15-21/), which simply updates the ITGE

602 estimation with revised pumping rates. More recently, Jiménez-Martínez et al. (2016) and Domingo-

603   Pinillos et al. (2018) report discharge values of 68 and 34.8 hm^3/yr, respectively. These values are closer to

604   the range suggested by our model.

605

606   We estimated nitrate discharge by weighting the discharge of groundwater with a spatial distribution of

607   nitrate concentration in the aquifer. On average, the aquifer discharged 10.2 Mkg/yr into the lagoon during

608   the studied period. This value is in good agreement with a previous evaluation of nitrate discharge of ~13.6

609   Mkg/yr caused by a groundwater discharge of 68 hm^3/yr (García-Aróstegui et al., 2017). An average nitrate

610   discharge of 10.2 Mkg/yr may sound high, but is realistic given the dimensions of the diffuse source term

611   (i.e., the irrigated area, 477 km^2) and the chemical load used in the intensive agriculture in the area (900–

612   1600 kg/ha/yr, Jiménez-Martínez et al., 2011) that lead to a total chemical input (mainly nitrate) of ~27–48

613   Mkg/yr. A second input of nitrate into the lagoon, not considered in this study, is surface water. For

614   example, Velasco et al. (2005) evaluated the surface discharge of nitrate at the mouth of the Rambla del

615   Albujón after the stormy period September 2002–October 2003 as 2 Mkg/yr. Bearing in mind that this

616   number summarizes a point discharge, a diffuse discharge of 10.2 Mkg/yr along a 30.3 km long coastline

617   cannot be viewed as an unrealistically high value. Ignoring water renewal, the degradation of nitrate and its

618   retention in the lacustrine sediments, a maximum nitrate concentration in the lagoon of ~7.5 mg/L can be

619   estimated. This upper bound is, indeed, larger than the measured nitrate concentrations (1 mg/L in the centre

620   of the lagoon, but 3.7 mg/L near the coast; Baudron et al., 2015; Velasco et al, 2005; DGA-MAGRAMA,

621   2018), but still in good agreement.

622

623   Despite the inherent uncertainties associated with any model (especially the first version of a novel model),

624   the reconstruction of the aquifer hydrodynamics towards the current state allows an explanation of the

625   recent algal blooms observed in the coastal lagoon. The large peak in nitrate concentration following a

626   severe storm (the strongest in 16 years) is clearly observable in Figure 10. This almost immediate response

627   of the aquifer can be easily explained by observing its history. Algal blooms did not occur in the period

628 2000–2008, when nitrate discharge into the lagoon was in the order of 25,000 kg/d or below. However, the

629 exceptionally wet period (end 2008–mid 2010) along with the permanent increase of nitrate concentration

630 in the aquifer (Figure 3) resulted in a rise and posterior stabilization of discharge of nitrates into the lagoon

631 with rate ~34,000 kg/d (end 2009–end 2013). Although discharge of both groundwater and nutrients have

632 showed decreasing trends in recent years, a high load of nutrients in the aquifer has been reached nowadays.

633 Since mid 2015, intense rainfall storm events like those at the end of December 2016 trigger high pulses of

634 nutrient inputs into the lagoon, with consequent anoxic conditions and algal bloom episodes that cause

635 death of the lagoon's biota (see e.g., DGA-MAGRAMA, 2018). The values of nitrate discharge presented

636 in this paper are upper bounds due to the many factors controlling the discharge of nutrients into the lagoon

637 that have been disregarded, e.g., (1) denitrification and phosphorus retention of the upper part of the aquifer

638 underlying the wetlands along the coastline (Velasco et al., 2006; Tercero et al., 2017), (2) temperature

639 fluctuations in the aquifer, and (3) connectivity with the Mediterranean Sea that controls water renewal in

640 the lagoon. The contribution of the surface drainage network has also been ignored, e.g., (1) acid drainage

641 from the abandoned Cartagena-La Unión mining district, (2) spills of urban effluents (especially during and

642 shortly after intense rainfall events, Velasco et al., 2005) that contribute nitrates together with other

643 nutrients such as additional phosphates, and (3) the flush of nitrates in the surface (Esteve Selma et al.,

644 2016).

645

646 Our numerical model helps to understand the past and to know the present of the Campo de Cartagena

647 plain–Mar Menor coastal lagoon system, but also to forecast its future state. In this paper, three plausible

648 management scenarios aimed at reducing the nutrient load into the lagoon were explored. The localized

649 scenarios involving drains are efficient to reduce the discharge of groundwater into the lagoon, provided

650 that current or projected basic pumping rates at drains are substantially increased. In fact, only the scenario

651 that includes the construction of new drains and with very high pumping rates is able to reduce the nitrate

652 discharge below 25,000 kg/d. The drawback of the localized scenarios is the risk of seawater intrusion

653 (inversion of flow regime) during dry periods, which would increase the desalinization costs for irrigation

654 and cause other environmental problems. Instead, the distributed scenario, which could be considered as a

655 complementary strategy to the current pumping existing drains, would also satisfy the water requirements

656 of crops and reduce the dependency of water resources provided by the inter-basin T-S WT. Assuming a

657 distributed pumping rate of ~15 hm^3/year, the reduction in the discharge of groundwater into the lagoon

658 would be still small. However, the reduction in the nitrate load into the lagoon would be considerable

659 (~2000 kg/d). Most likely, a combination of the localized and distributed scenarios is necessary to achieve

660 a sustainable regime of the Campo de Cartagena plain–Mar Menor coastal lagoon system.

661

662 **5. Concluding remarks**

663 The system Campo de Cartagena plain-Mar Menor coastal lagoon is a characteristic example of a highly-

664 modified and anthropized hydro-ecosystem. Multiple pressures and associated impacts on the lagoon are a

665 direct consequence of intensive exploitation of the landscape. The current significant ecological

666 deterioration of the lagoon makes it necessary and urgent to adopt integrated and sustainable management

667 strategies to alleviate pressures on the system, and to enhance the resilience of the region against future

668 scenarios of land use and climate change.

669

670 In spite of the considerable efforts over the last decades to improve the understanding of the interaction

671 between the Campo de Cartagena plain and the Mar Menor coastal lagoon, there was a major gap regarding

672 the underground connection, which has a considerable impact on both the vulnerability of the lagoon and

673 on the availability of groundwater resources inland. In this study, we have presented an integrated 3D

674 hydrogeological model that couples a surface hydrology model with a groundwater model. A reconstruction

675 over sixteen years (2000-2016) of the system hydrodynamics reveals clear-cut links between groundwater

676 inputs and observed algal blooms in the lagoon. The discharge of groundwater and nitrates presented in this

677 paper provides an upper bound for the actual amounts due to model limitations caused by lack of

678 information.

679

680   The calibrated model was used to simulate mitigation alternatives aimed at reducing the discharge of

681   nutrients into the lagoon to ensure its ecologic health. Three scenarios involving pumping from drains and

682   distributed pumping have been proposed. All three are able to reduce the discharge of groundwater into the

683   lagoon and, correspondingly, the discharge of nitrate, assumed to be one of the main responsibles of algal

684   blooms. Unfortunately, none is capable of maintaining the mass flux of nitrate below tolerable levels.

685   Likely, a combination of pumping from drains (localized scenarios) and distributed pumping from inland

686   wells (distributed scenario) would provide a viable solution. None the less, the spatio-temporal

687   quantification of groundwater discharge presented in this paper is a valuable tool for the design of new

688   management alternatives and their evaluation.

689

690   Despite the model is able to accurately reproduce the recent history of the aquifer, much remains to be done.

691   Because of its novelty and early development stage, some uncertainties still remain unresolved and should

692   be coped in upcoming exercises. Uncertainties mostly arise from (1) the scarcity of measurements available

693   to model calibration (of both heads and model parameters), and (2) the lack of information about aquifer's

694   sink terms, i.e., the vertical transfer of groundwater to deeper aquifers through leaky wells and localized

695   groundwater pumping. Improvements to the model are expected to better narrow the range of discharge

696   into the lagoon, and to accurately quantify the source of irrigation water and the interactions between

697   shallow and deeper aquifers. Climate change scenarios, which clearly impact on the recharge patterns, or

698   other management strategies, e.g. optimization of adaptive pumping along the coastline or surface water-

699   groundwater conjunctive use, may also be simulated in upcoming exercises. The modelling exercise

700   presented here must be viewed as a first and hopeful step in the direction of achieving a more integrated

701   and holistic water management scheme for the sustainability of the Campo de Cartagena-Mar Menor lagoon

702   agroecosystem.

703

704

714

715 **References**

716 Alcolea A., Carrera J., Medina A. (2006). Pilot points method incorporating prior information for solving

717   the groundwater flow inverse problem. *Adv. Water Resour.,* 29: 1678-1689.

718 Alcon, F., de Miguel, M. D., and Burton, M. (2011). Duration analysis of adoption of drip irrigation

719   technology in southeastern Spain. *Technol. Forecast. Soc. Change*, 78(6): 991-1001.

720   doi:10.1016/j.techfore.2011.02.001.

721 Aparicio, J., Candela, L., Alfranca, O., and García-Aróstegui, J. L. (2017). Economic evaluation of small

722   desalination plants from brackish aquifers. Application to Campo de Cartagena (SE Spain).

723   *Desalination*, 411: 38-44.

724 Arellano-Aguilar, O., Betancourt-Lozano, M., Aguilar-Zárate, G., and de Leon-Hill, C. P. (2017).

725   Agrochemical loading in drains and rivers and its connection with pollution in coastal lagoons of the

726   Mexican Pacific. *Environ. Monit. Assess.*, 189(6): 270.

727 Ascott, M. J., Gooddy, D. C., Wang, L., Stuart, M. E., Lewis, M. A., Ward, R. S. and Binley, A. M. (2017).

728   Global patterns of nitrate storage in the vadose zone. *Nat. Comm.*, *8*(1), 1416.

729   Baudron, P., Barbecot, F., Gillon, M., Garcia-Arostegui, J. L., Travi, Y., Leduc, C., Gomariz Castillo, F.

730   and Martinez-Vicente, D. (2013). Assessing groundwater residence time in a highly anthropized

731   unconfined aquifer using bomb peak C-14 and reconstructed irrigation water H-3. *Radiocarbon*, 55:

732   993-1006. doi:10.2458/azu_js_rc.55.16396.

733   Baudron, P., Cockenpot, S., Lopez-Castejon, F., Radakovitch, O., Gilabert, J., Mayer, A., Garcia-Arostegui,

734   J. L., Martinez-Vicente, D., Leduc, C., and Claude, C. (2015). Combining radon, short-lived radium

735   isotopes and hydrodynamic modeling to assess submarine groundwater discharge from an anthropized

736   semiarid watershed to a Mediterranean lagoon (Mar Menor, SE Spain). *J. Hydrol.*, 525: 55-71.

737   Boynton, W. R., Murray, L., Hagy, J. D., Stokes, C., and Kemp, W. M. (1996). A comparative analysis of

738   eutrophication patterns in a temperate coastal lagoon. *Estuaries*, 19(2): 408-421.

739   Breininger, D. R., Breininger, R. D., and Hall, C. R. (2017). Effects of surrounding land use and water

740   depth on seagrass dynamics relative to a catastrophic algal bloom. *Conserv. Biol.*, 31(1): 67-75.

741   Candela, L., Elorza, F. J., Tamoh, K., Jiménez-Martínez, J., and Aureli, A. (2013). Groundwater modelling

742   with limited data sets: the Chari-Logone area (Lake Chad Basin, Chad). *Hydrol. Process.*, doi:

743   10.1002/hyp.9901

744   Contreras, S., Hunink, J. E., and Baille, A. (2014). Building a watershed information system for the Campo

745   de Cartagena basin (Spain) Integrating hydrological modeling and remote sensing. FutureWater Report

746   125, 59 pp. Cartagena, Spain. Available from www.futurewater.es.

747   Contreras, S., Alcolea, A., Jiménez-Martínez, J., and Hunink, J. (2017). Cuantificación de la descarga

748   subterránea al Mar Menor mediante modelización hidrogeológica del acuífero superficial cuaternario.

749   FutureWater Report 176, 89 pp. Available from www.futurewater.es.

750   DGA-MAGRAMA (2018). Análisis de soluciones para el objetivo del vertido cero al Mar Menor

751   proveniente del Campo de Cartagena. Ministerio de Agricultura, Pesca, Alimentación y Medio

752   Ambiente, Madrid (Spain). At http://www.mapama.gob.es/es/agua/participacion-publica/ (Mar Menor-

753   Campo de Cartagena).

754 Dimova, N., Ganguli, P. M., Swarzenski, P. W., Izbicki, J. A., and O'Leary, D. (2017). Hydrogeologic

755 controls on chemical transport at Malibu Lagoon, CA: Implications for land to sea exchange in coastal

756 lagoon systems. *J. Hydrol.: Regional Studies*, 11: 219-233.

757 Doherty, J. (2016). PEST-model-independent parameter estimation. User manual part I, 6th edn.

758 Watermark Numerical Computing, Brisbane, pp. 318.

759 Domingo-Pinillos, J. C., Senent-Aparicio, J., García-Aróstegui, J. L., and Baudron, P. (2018). Long term

760 hydrodynamic effects in a semi-arid mediterranean multilayer aquifer: Campo de

761 Cartagena in south-eastern Spain. *Water*, 10 (1320). doi:10.3390/w10101320.

762 Duck, R. W., and da Silva, J. F. (2012). Coastal lagoons and their evolution: A hydromorphological

763 perspective. *Estuar. Coast. Shelf Sci.*, 110: 2-14.

764 Esteve Selma, M. A., Martínez Martínez, J., Fitz, C., Robledano, F., Martínez Paz, J. M., Carreño, M. F.,

765 Guaita, N., Martínez López, J., and Miñano, J. (2016). Environmental Conflicts Deriving From Land-

766 Use Intensification in the Mar Menor Watershed: an Inter-Disciplinary Approach. *In*: IEO Temas de

767 Oceanografía, 9: Mar Menor un ecosistema singular. Evaluación científica del pasado, presente y futuro

768 de la laguna costera (Eds. V.M. León and J.M. Bellido). Chapter 3. IEO, Murcia, Spain. 79-110.

769 García-Aróstegui, J. L., Marín Arnaldos, F., and Martínez Vicente, D. (2017). Informe integral sobre el

770 estado ecológico del Mar Menor, 1. Hidrogeología. Ed. Región de Murcia & Espacios Naturales Región

771 de Murcia.

772 Garcia-Oliva, M., Perez-Ruzafa A., Umgiesser, G., McKiver, W., Ghezzo, M., De Pascalis, F., and Marcos,

773 C. (2018). Assessing the hydrodynamic response of the Mar Menor lagoon to dredging inlets

774 interventions through numerical modelling. *Water*, 10 (959). doi:10.3390/w10070959.

775 Garcia-Pintado, J., Martinez-Mena, M., Barbera, G. G., Albaladejo, J., and Castillo, V. M. (2007).

776 Anthropogenic nutrient sources and loads from a Mediterranean catchment into a coastal lagoon: Mar

777 Menor, Spain. *Sci. Total Environ.,* 373: 220-239. doi:10.1016/j.scitotenv.2006.10.046.

778 Gilmore, T. E., Genereux, D. P., Solomon, D. K., Farrell, K. M., and Mitasova, H. (2016). Quantifying an

779 aquifer nitrate budget and future nitrate discharge using field data from streambeds and well nests. *Water*

780 *Resour. Res.*, 52(11): 9046-9065.

781 Han, D., Currell, M. J., Cao, G., and Hall, B. (2017). Alterations to groundwater recharge due to

782 anthropogenic landscape change. *J. Hydrol.*, 554: 545-557.

783 Hunink, J. E., Contreras, S., Soto-García, M., Martin-Gorriz, B., Martinez-Álvarez, V., and Baille, A.

784 (2015). Estimating groundwater use patterns of perennial and seasonal crops in a Mediterranean

785 irrigation scheme, using remote sensing. *Agric. Water Manag.*, 162: 47-56.

786 Isla, F. I. (1995). Coastal lagoons. In Developments in Sedimentology (Vol. 53, pp. 241-272). Elsevier.

787 ITGE (1991). Estudio Hidrogeológico del Campo de Cartagena (2ª Fase). Volume 1/2 Memory. Volume

788 2/2 Annex 1, 2, 3 and 4. Technical report. Geological Survey of Spain, Madrid, Spain, 131 pp.

789 Jimenez-Carceles, F. J., and Alvarez-Rogel, J. (2008). Phosphorus fractionation and distribution in salt

790 marsh soils affected by mine wastes and eutrophicated water: A case study in SE Spain. *Geoderma*, 144:

791 299-309. doi:10.1016/j.geoderma.2007.11.024.

792 Jiménez-Martínez, J. (2010). Aquifer recharge from intensively irrigated farmland: several approaches.

793 Ph.D. Dissertation. Pub. Technical University of Catalonia, ISBN: 9788469370452.

794 Jiménez-Martínez, J., Candela, L., Molinero, J., and Tamoh, K. (2010). Groundwater recharge in irrigated

795 semi-arid areas with different crops. Quantitative hydrological modelling and sensitivity analysis.

796 *Hydrogeol. J.*, 18: 1811-1824. doi:10.1007/s10040-010-0658-1.

797 Jiménez-Martínez, J., Aravena, R., and Candela, L. (2011). The role of leaky boreholes in the contamination

798 of a regional confined aquifer. A case study: The Campo de Cartagena region, Spain. *Water Air Soil*

799 *Pollut.,* 215: 311-327. doi:10.1007/s11270-010-0480-3.

800 Jiménez-Martínez, J., Candela, L., García-Aróstegui, J. L., and Aragon, R. (2012). A 3D geological model

801 of Campo de Cartagena, SE Spain: Hydrogeological implications. *Geol. Acta*, 10: 49-62.

802 doi:10.1344/105.000001703.

803 Jiménez-Martínez, J., García-Aróstegui, J.L., Hunink, J., Contreras, S., Baudron, P., and Candela, L.
804   (2016). The role of groundwater in highly human-modified hydrosystems: A review of impacts and
805   mitigation options in the Campo de Cartagena-Mar Menor coastal plain (SE Spain). *Environ. Rev.*,
806   doi:10.1139/er-2015-0089.

807 Kjerfve, B. (1994). Coastal lagoons. In Elsevier oceanography series (Vol. 60, pp. 1-8). Elsevier.

808 Lapuente, E. (2012). Full cost in desalination. A case study of the Segura River Basin. *Desalination*, 300:
809   40-45. doi:10.1016/j.desal.2012.06.002.

810 Le Moal, M., Gascuel-Odoux, C., Ménesguen, A., Souchon, Y., Étrillard, C., Levain, A., Moatar, F.,
811   Pannard, A., Souchu, P., Lefebvre, A. and Pinay, G. (2019). Eutrophication: A new wine in an old
812   bottle?. *Sci. Tot. Environ.*, 651: 1-11.

813 Lee, V., and Olsen, S. (1985). Eutrophication and management initiatives for the control of nutrient inputs
814   to Rhode Island coastal lagoons. *Estuaries*, 8(2): 191-202.

815 Marcos, C., Torres, I., Lopez-Capel, A., and Perez-Ruzafa, A. (2015). Long term evolution of fisheries in
816   a coastal lagoon related to changes in lagoon ecology and human pressures. *Rev. Fish Biol. Fish.,* 25(4):
817   689-713. doi:10.1007/s11160-015-9397-7.

818 Martin-Gorriz, B., Soto-Garcia, M., and Martinez-Alvarez, V. (2014). Energy and greenhouse-gas
819   emissions in irrigated agriculture of SE (southeast) Spain. Effects of alternative water supply scenarios.
820   *Energy*, 77: 478-488. doi:10.1016/j.energy.2014.09.031.

821 McCrackin, M. L., Jones, H. P., Jones, P. C., and Moreno-Mateos, D. (2017). Recovery of lakes and coastal
822   marine ecosystems from eutrophication: A global meta-analysis. *Limnol. Oceanogr.*, 62(2): 507-518.

823 Meier, P. M., Carrera, J., and Sanchez-Vila, X. (1999). A numerical study on the relationship between
824   transmissivity and specific capacity in heterogeneous aquifers. *Groundwater*, 37(4): 611-617.

825 Mencló, A., Casamitjana, X., Mas-Pla, J., Coll, N., Compte, J., Martinoy, M., Pascual, J., and Quintana, X.
826   D. (2017). Groundwater dependence of coastal lagoons: The case of La Pletera salt marshes (NE
827   Catalonia). *J. Hydrol.*, 552: 793-806.

828 Mesnage, V., and Picot, B. (1995). The distribution of phosphate in sediments and its relation with

829   eutrophication of a Mediterranean coastal lagoon. *Hydrobiologia*, 297(1): 29-41.

830 Moreno-Gonzalez, R., Rodriguez-Mozaz, S., Gros, M., Barcelo, D., and Leon, V. M. (2015). Seasonal

831   distribution of pharmaceuticals in marine water and sediment from a mediterranean coastal lagoon (SE

832   Spain). *Environ. Res.,* 138: 326-344. doi:10.1016/j.envres.2015.02.016.

833 Nakamura, Y., and Kerciku, F. (2000). Effects of filter-feeding bivalves on the distribution of water quality

834   and nutrient cycling in a eutrophic coastal lagoon. *J. Mar. Syst.*, 26(2): 209-221.

835 Naldi, M., and Viaroli, P. (2002). Nitrate uptake and storage in the seaweed Ulva rigida C. Agardh in

836   relation to nitrate availability and thallus nitrate content in a eutrophic coastal lagoon (Sacca di Goro,

837   Po River Delta, Italy). *J. Exp. Mar. Biol. Ecol.*, 269(1): 65-83.

838 Newton, A., Icely, J. D., Falcão, M., Nobre, A., Nunes, J. P., Ferreira, J. G., and Vale, C. (2003). Evaluation

839   of eutrophication in the Ria Formosa coastal lagoon, Portugal. *Cont. Shelf Res.*, 23(17-19): 1945-1961.

840 Pérez-Cutillas, P., (2013). Modelización de propiedades físicas del suelo a escala regional. Casos de estudio

841   en el Sureste Ibérico. PhD Thesis. Universidad de Murcia, Murcia, Spain, 374 pp.

842 Perez-Ruzafa, A., Marcos, C., Perez-Ruzafa, I. M., Barcala, E., Hegazi, M. I., and Quispe, J. (2007).

843   Detecting changes resulting from human pressure in a naturally quick-changing and heterogeneous

844   environment: Spatial and temporal scales of variability in coastal lagoons. *Estuar. Coast. Shelf Sci.,* 75:

845   175-188. doi:10.1016/j.ecss.2007.04.030.

846 Perez-Ruzafa, A., Marcos, C., and Perez-Ruzafa, I. M. (2009). 30 años de estudios en la laguna costera del

847   Mar Menor: de la descripción del ecosistema a la comprensión de los procesos y la solución de los

848   problemas ambientales. *In* Fundación Instituto Euromediterráneo del Agua. *Edited by* El Mar Menor.

849   Estado actual del conocimiento científico. Murcia, Spain. pp. 17-46.

850 Perez-Ruzafa, A., Marcos, C., and Perez-Ruzafa, I. M. (2011). Mediterranean coastal lagoons in an

851   ecosystem and aquatic resources management context. *Phys. Chem. Earth*, 36: 160-166.

852   doi:10.1016/j.pce.2010.04.013.

853   Perez-Ruzafa, A., Marcos, C., Perez-Ruzafa, I. M., and Perez-Marcos, M. (2013). Are coastal lagoons

854   physically or biologically controlled ecosystems? Revisiting r vs. K strategies in coastal lagoons and

855   estuaries. *Estuar. Coast. Shelf Sci.,* 132: 17-33. doi:10.1016/j.ecss.2012.04.011.

856   Robinson, C. E., Xin, P., Santos, I. R., Charette, M. A., Li, L., and Barry, D. A. (2017). Groundwater

857   dynamics in subterranean estuaries of coastal unconfined aquifers: Controls on submarine groundwater

858   discharge and chemical inputs to the ocean. *Adv. Water Resour.,* 115: 315-331.

859   Rodellas, V., Garcia-Orellana, J., Masqué, P., Feldman, M., and Weinstein, Y. (2015). Submarine

860   groundwater discharge as a major source of nutrients to the Mediterranean Sea. *Proc. Nat. Acad. Sci.*,

861   112(13): 3926-3930.

862   Rodríguez-Gallego, L., Achkar, M., Defeo, O., Vidal, L., Meerhoff, E., and Conde, D. (2017). Effects of

863   land use changes on eutrophication indicators in five coastal lagoons of the Southwestern Atlantic

864   Ocean. *Estuar. Coast. Shelf Sci.*, 188: 116-126.

865   Sanchez, M. I., Lopez, F., Del Amor, F., and Torrecillas, A. (1989). La evaporación y evapotranspiración

866   en el Campo de Cartagena y Vega Media del Segura. Primeros resultados. *Anales Edafologia Agrobiol.*:

867   1239-1251.

868   Sánchez-Badorrey, E. and Jalón-Rojas, I. (2015). A New Method for Zoning of Coastal Barriers based on

869   Hydro-geomorphological and Climate Criteria. *Int. J. Environ. Res.*, 9(1): 351-362.

870   Santos, I. R., Eyre, B. D., and Huettel, M. (2012). The driving forces of porewater and groundwater flow

871   in permeable coastal sediments: A review. *Estuar. Coast. Shelf Sci.*, 98: 1-15.

872   Shapiro, A. M. (2007). Publishing our "ugly babies". *Groundwater* 45(6). doi:10.1111/j.1745-

873   6584.2007.00351.x.

874   Shokri, N., and Or, D. (2011). What determines drying rates at the onset of diffusion controlled stage-2

875   evaporation from porous media?. *Water Resour. Res.*, 47(9). doi:10.1029/2010WR010284.

876   Tercero, M. C., Álvarez-Rogel, J., Conesa, H. M., Párraga-Aguado, I., and González-Alcaraz, M. N. (2017).

877   Phosphorus retention and fractionation in an eutrophic wetland: A one-year mesocosms experiment

878   under fluctuating flooding conditions. *J. Environ. Manage.*, 190: 197-207.

879   Terink, W., Lutz, A. F., Simons, G. W. H., Immerzeel, W. W., and Droogers, P. (2015). SPHY v2.0: Spatial

880   Processes in HYdrology. *Geosci. Model Dev.,* 8: 2009-2034. doi:10.5194/gmd-8-2009-2015

881   Thiem, G., Hydrologische Methoden. Ph.D. Dissertation, TU Stuttgart. Gebhardt Pub., Leipzig, 1906.

882   Tragsatec (2013). Informe hidrogeológico de la red de drenaje de aguas salobres del Campo de Cartagena.

883   Traverso-Soto, J. M., Lara-Martín, P. A., González-Mazo, E., and León, V. M. (2015).

884   Distribution of anionic and nonionic surfactants in a sewage-impacted Mediterranean coastal lagoon:

885   Inputs and seasonal variations. *Sci. Total Environ.* 503: 87-96. doi:10.1016/j.scitotenv.2014.06.107.

886   Velasco, J., Lloret, J., Millan, A., Barahona, J., Abellan, P., and Sanchez-Fernandez, D. (2006). Nutrient

887   and particulate inputs into the Mar Menor lagoon (SE Spain) from an intensive agricultural watershed.

888   *Water Air Soil Pollut.* 176: 37-56. doi: 10.1007/s11270-006-2859-8.

889   Vero, S. E., Basu, N. B., Van Meter, K., Richards, K. G., Mellander, P. E., Healy, M. G., and Fenton, O.

890   (2018). The environmental status and implications of the nitrate time lag in Europe and North America.

891   *Hydrogeol. J.*, 26(1): 7-22.

892   Villalobos, F. J., Orgaz, F., and Fereres, E. (2006). Estudio sobre las necesidades de agua de riego de los

893   cultivos en la zona del trasvase Tajo-Segura. Murcia, Spain.

894   Voss, C. I., and Provost, A. M. (2010). SUTRA, A model for saturated-unsaturated variable-density ground-

895   water flow with solute or energy transport, U.S. Geological Survey Water-Resources Investigations

896   Report 02-4231, 291 p.

897   Werner, A. D., Bakker, M., Post, V. E., Vandenbohede, A., Lu, C., Ataie-Ashtiani, B., Simmons, C. T. and

898   Barry, D. A. (2013). Seawater intrusion processes, investigation and management: recent advances and

899   future challenges. *Adv. Water Resour.*, 51: 3-26.

900   Wösten, J. H. M., Pachepsky, Y., and Rawls, W. J. (2001). Pedotransfer functions: bridging the gap between

901   available basic soil data and missing soil hydraulic characteristics. *J. Hydrol.,* 251: 123-150.

902   doi:10.1016/S0022-1694(01)00464-4.

903   Yu, X., Xin, P., Lu, C., Robinson, C., Li, L., and Barry, D. A. (2017). Effects of episodic rainfall on a

904   subterranean estuary. *Water Resour. Res.*, 53: 5774-5787. doi:10.1002/2017WR020809.

905   **Tables**

906

907   **Table 1.** Mean values of the water balance components in the Quaternary aquifer, and nitrate load released

908   into the lagoon for wet, average and dry hydrometeorological periods, and for the complete 16-year study

909   period. All values are direct model outputs, except those italicized, which represent the estimated discharge

910   of nitrate if the vertical fluxes to deeper aquifers and the pumping from the shallow aquifer (overall 30–

911   40% of the recharge) are taken into account. The nitrate discharge in the presence of vertical fluxes and

912   pumping were estimated using the mean NO_3^- concentration in monitored wells (dashed grey line in Figure

913   3).

	Wet period	Average period	Dry period	All periods
	(Sep. 2008–Aug. 2010)	(Apr. 2002–Mar. 2004)	(Sep. 2013–Aug. 2015)	(Oct. 2000–Dec. 2016)
Recharge (hm^3/yr)	233.3	62.3	12.2	83.6
Discharge (hm^3/yr)	84.9	80.9	69.5	78.3 *53.3[a] – 44.9[b]*
Drains (hm^3/yr)	0.5	NA[*]	0.9	0.4
Storage variation (hm^3/yr)	147.9	-18.6	-58.2	4.9
Nitrate discharge (Mkg/yr)	11.8	8.2	11.4	10.2 *6.9[a] – 5.9[b]*

[*]: Drains operational since 2008.

a, *b*: Values corresponding to vertical fluxes and pumping corresponding to 30% and 40% of the recharge, respectively.
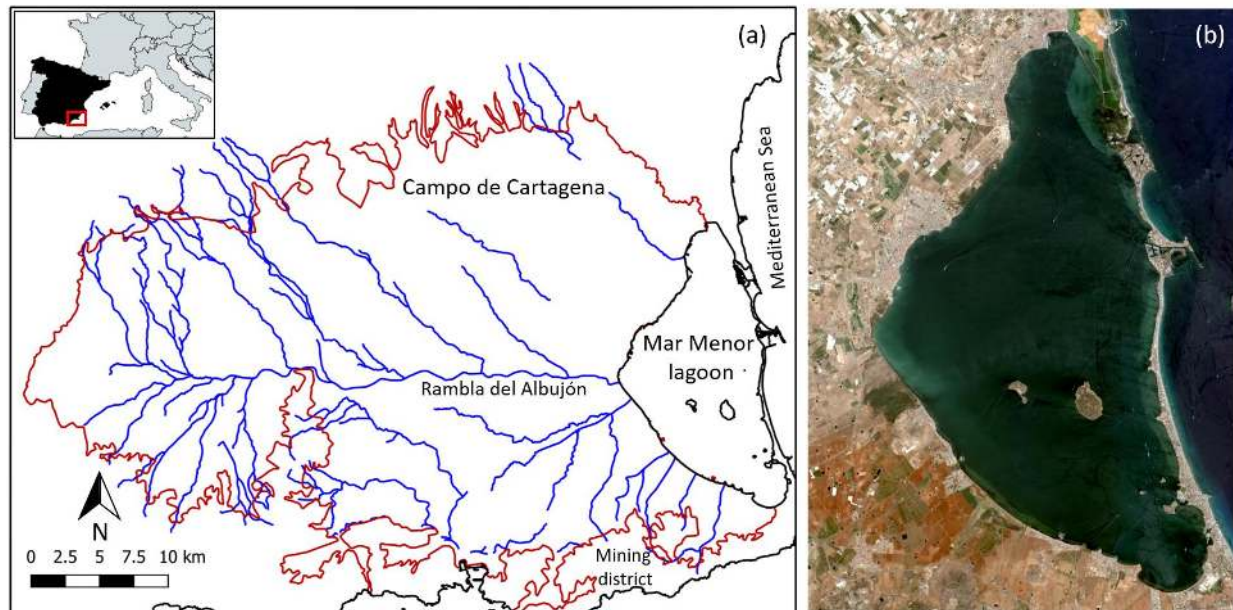
914
915
916
917

918

Figures

**Figure 1:** (a) The hydrogeological system of the Campo de Cartagena plain-Mar Menor coastal lagoon. The red line depicts the contour of the Quaternary aquifer (i.e., the limit of the groundwater flow model). The blue lines depict the watercourses that define the surface drainage network. For its relevance to this study, only the central watercourse "Rambla del Albujón" is labelled. The frame encompasses the surface water flow model; (b) Aerial view of the Mar Menor lagoon.
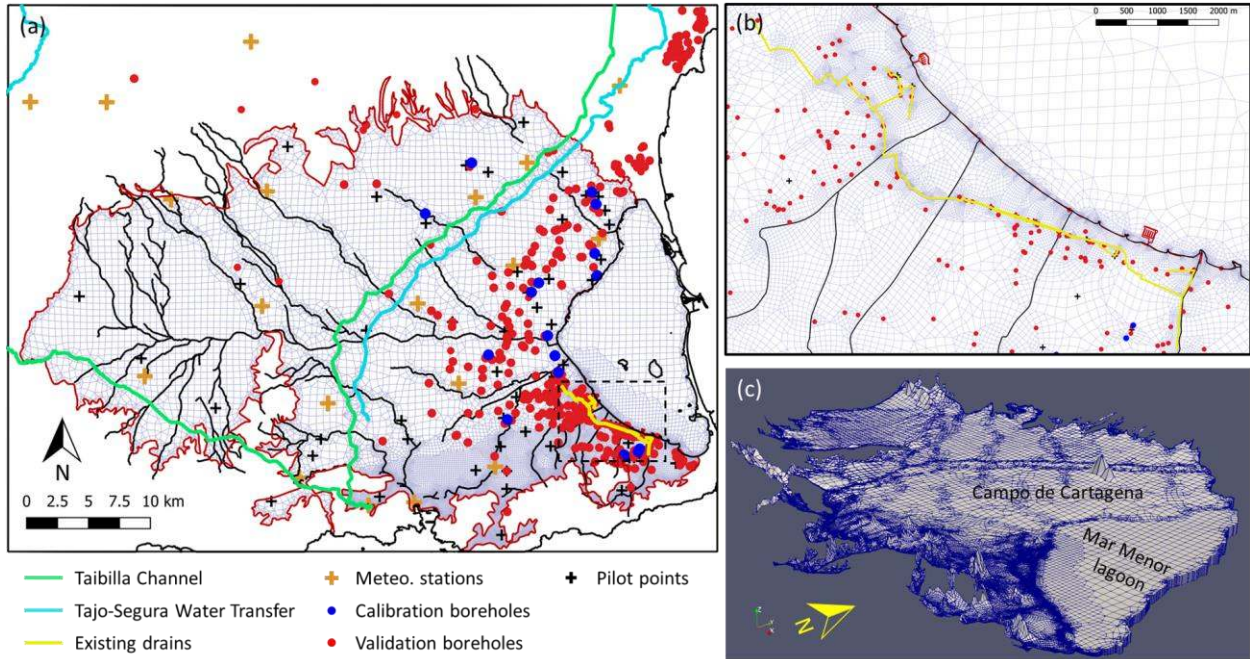
Figure 2: (a) The model set-up, including the surface water network, existing water transfers and drains, meteorological stations, observation boreholes for model calibration/validation and pilot points; (b) Detail of the fine model discretization in the vicinity of existing drains; (c) 3D view of model discretization (vertical exaggeration factor ×10).
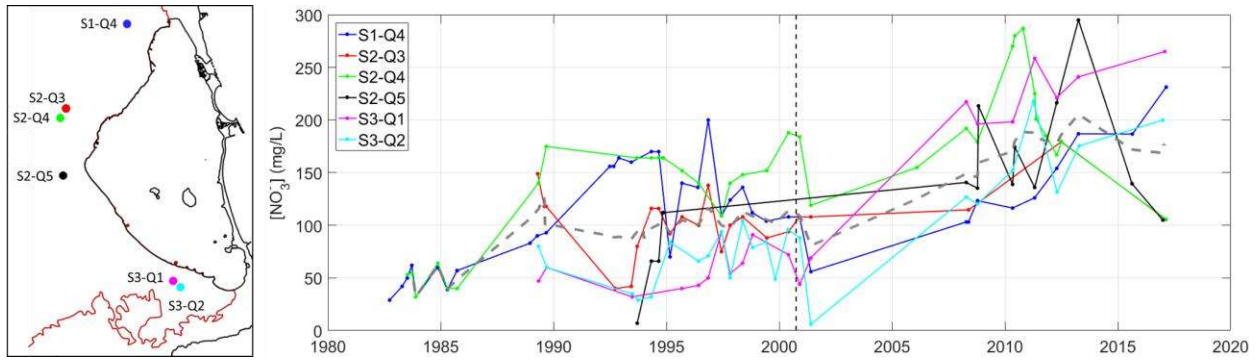
939

Figure 3: Location of wells where nitrate concentration is monitored (left) and the temporal evolution of nitrate concentration over the period 1980–2017 (right). The vertical dashed line depicts the beginning of the simulated period (October 2000). The grey dashed line depicts the mean concentration in monitored boreholes. Monitoring network: IGME-CHS.

944

945

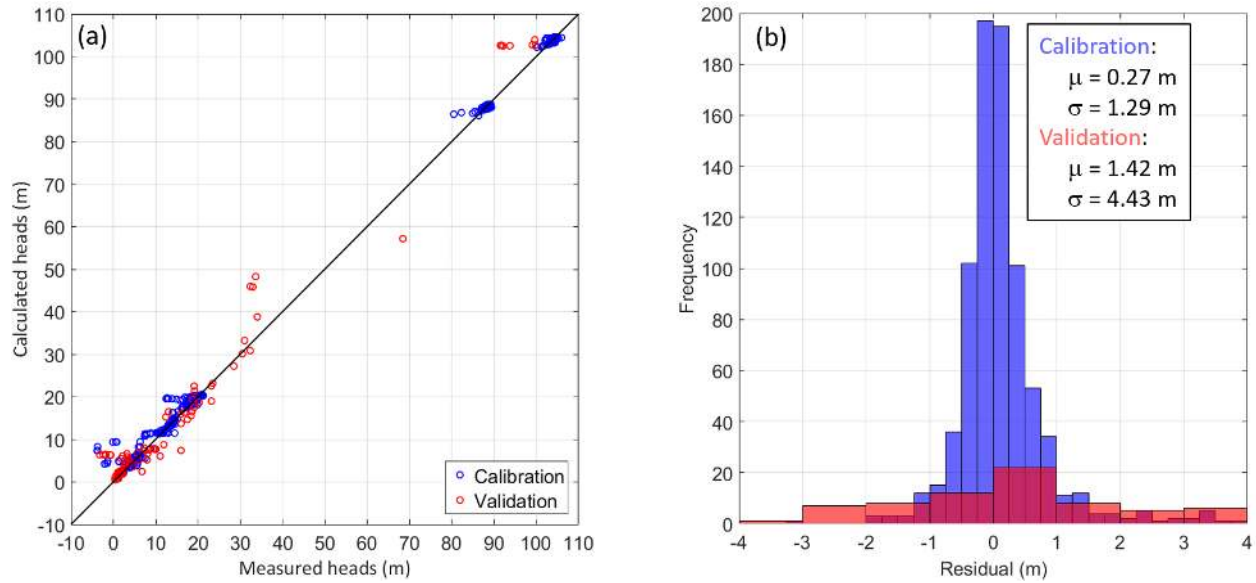946
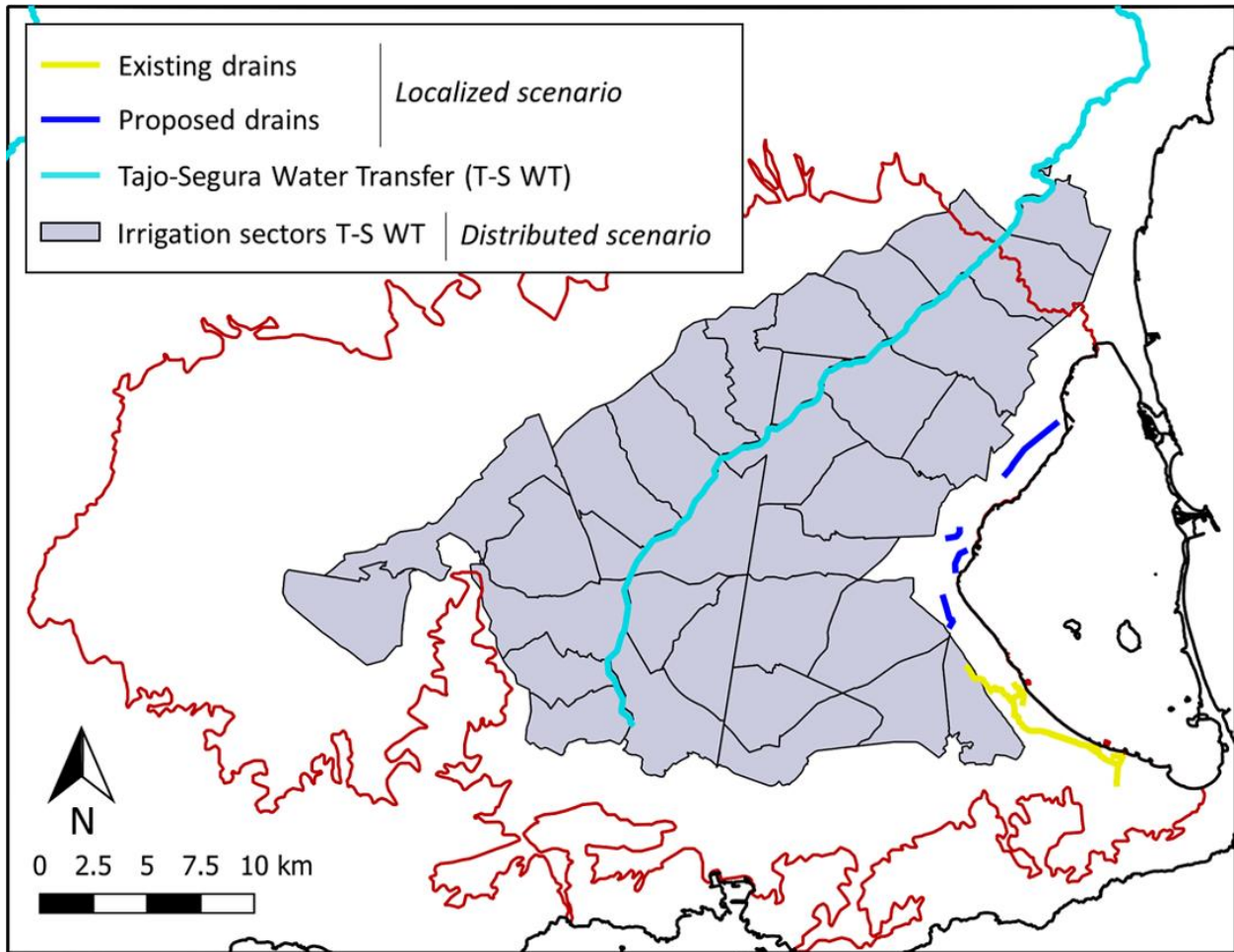
Figure 4: Localized and distributed management scenarios.

948

949

950

Figure 5: (a) Scatter plot of the measured and calculated hydraulic heads after the calibration (blue) and

951   validation exercises (red); (b) Histograms of residuals, defined as calculated minus measured

952

953   values. Note that fewer bins are used to define the histogram of residuals for the validation

954   exercise due to the reduced number of measurements. The inset gives the mean residual μ and

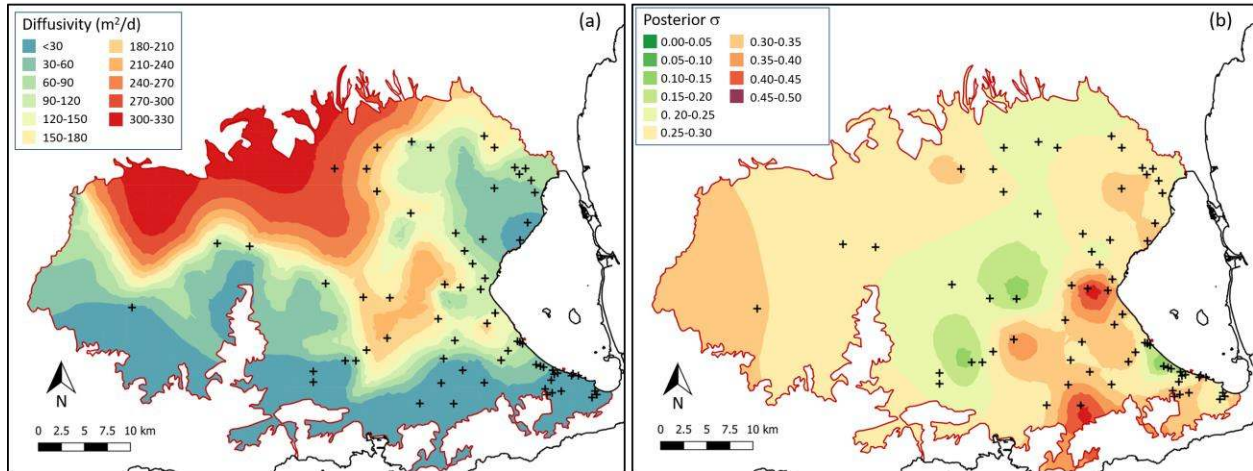955   standard deviation σ of the distribution of residuals.

956

957

958

959

960

Figure 6: (a) Spatial distribution of hydraulic diffusivity after calibration. The estimated mean diffusivity

of existing drains is ~500 m^2/d and is not displayed here to avoid distorting the colour scale. The

crosses depict the pilot points, where the estimation of model parameters is actually carried out.

Given the absence of information on model parameters in the lagoon, pilot points are located

inland only. Thus, estimated diffusivity values in the lagoon are highly uncertain and excluded

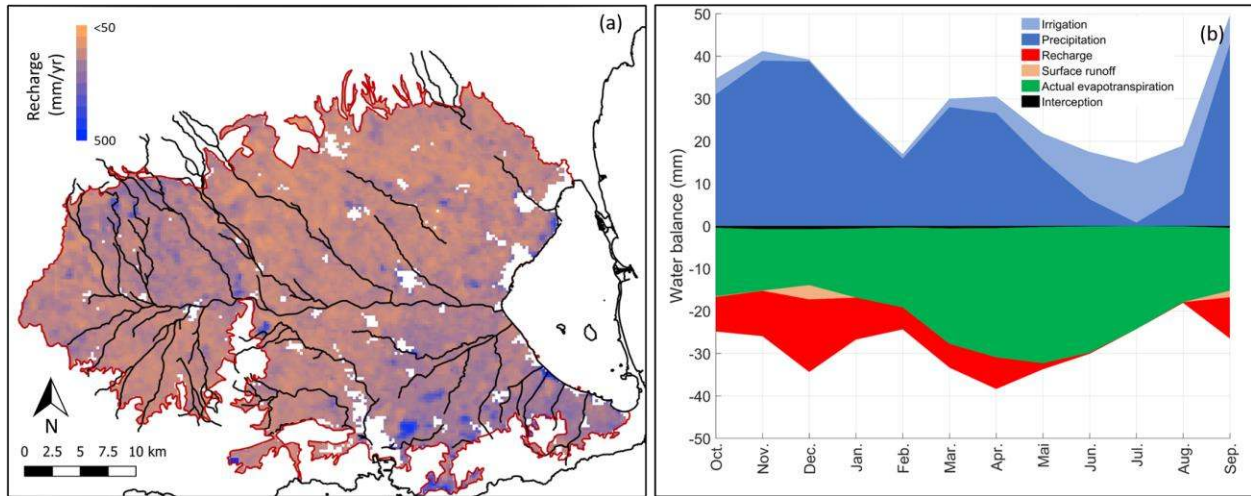from this plot; (b) Composite of posterior standard deviations of the estimated parameters.

Figure 7: (a) Spatial distribution of estimated mean annual recharge (mm/yr); (b) Monthly averaged water mass balance components for the study period (2000-2016), i.e., precipitation and irrigation as inflows, and actual evapotranspiration, surface runoff, interception and recharge as outflows.
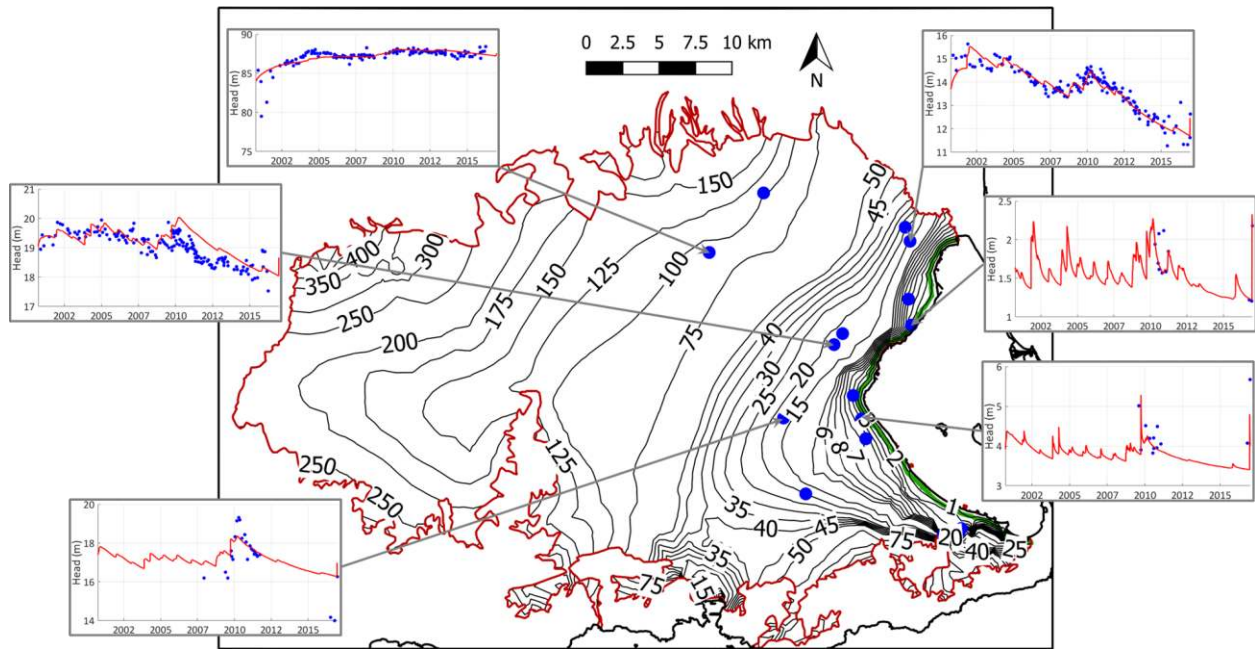
983

Figure 8: Contours of the hydraulic heads from the calibrated model at date 15/03/2004, after a two-year hydrometeorological average period: (1) head isolines (black lines; note that isolines are not equidistant); (2) mean penetration of the saltwater wedge at aquifer bottom (green line). The insets depict the temporal evolution of calculated hydraulic heads (red lines) and available measurements for model calibration (blue points) at selected observation wells.

989

	Wet period (Sept. 2008-Aug. 2010)		Average period (Apr. 2002-Mar. 2004)		Dry period (Sept. 2013-Aug. 2015)		Global mean (Oct. 2000-Dec. 2016)	
	% H$_2$O	% NO$_3^-$	% H$_2$O	% NO$_3^-$	% H$_2$O	% NO$_3^-$	% H$_2$O	% NO$_3^-$
North7	9.19	6.45	9.86	6.98	9.10	9.49	9.39	7.65
North6	12.18	8.55	13.12	9.29	12.27	12.79	12.56	10.24
North5	3.04	2.14	2.99	2.12	2.84	2.96	3.00	2.44
North4	0.41	0.29	0.31	0.22	0.22	0.23	0.32	0.25
North3	2.20	1.92	2.24	1.49	2.35	2.08	2.27	1.85
North2	12.69	11.06	12.77	8.51	13.60	12.03	12.96	10.60
North1	19.99	27.28	19.88	26.89	21.01	17.20	20.24	24.29
South1	24.82	25.08	24.67	29.12	25.66	28.03	25.05	26.85
South2	9.04	9.14	8.88	10.49	8.99	9.82	8.97	9.61
South3	3.22	4.10	2.67	2.53	2.22	3.07	2.71	3.29
South4	2.14	2.72	1.77	1.68	1.10	1.53	1.69	2.00
South5	0.82	1.04	0.63	0.60	0.42	0.58	0.62	0.75
South6	0.19	0.17	0.15	0.06	0.15	0.14	0.17	0.13
South7	0.03	0.02	0.03	0.01	0.03	0.03	0.03	0.02
South8	0.03	0.03	0.03	0.01	0.04	0.03	0.03	0.03

990

Figure 9: Spatio-temporal distribution of discharge of groundwater and nitrate into the Mar Menor lagoon. The perimeter of the lagoon is divided into 15 segments with length ~2 km. For each segment, the discharge of groundwater (solid lines) and nitrate (dashed line with same colour) are presented. Periods of average (grey), wet (blue), and dry (red) hydrometeorological conditions are highlighted. The table contains, for each sector, the percentage of the mean discharge of groundwater (%H$_2$0) and nitrates (%NO$_3^-$) for selected hydrometeorological periods.

997
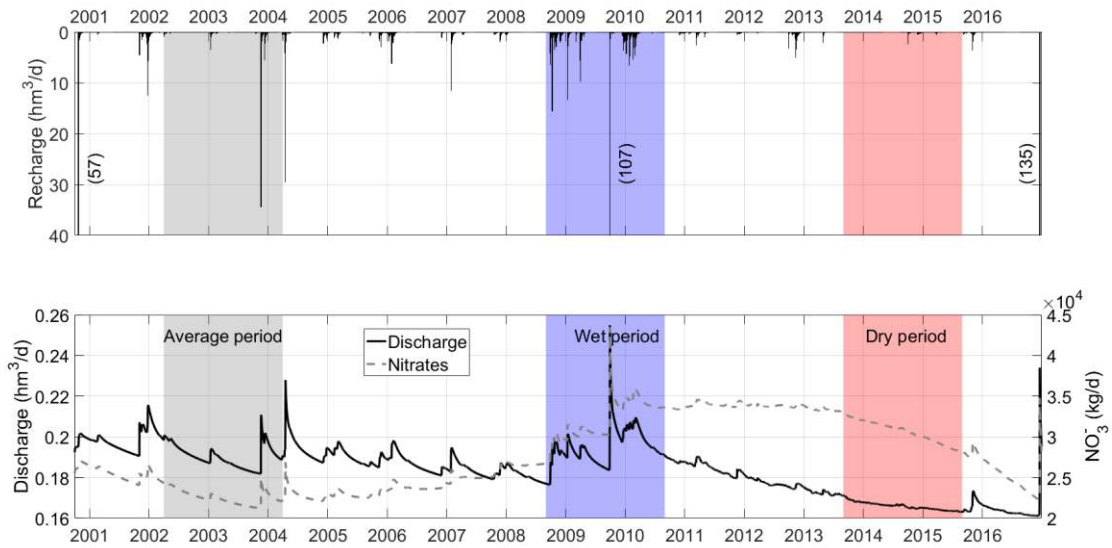
998

999   **Figure 10:** (a) Daily total recharge over the entire aquifer estimated by SPHY. The vertical axis has been

1000   trimmed to show the variation among the smaller recharge peaks. Values in parentheses
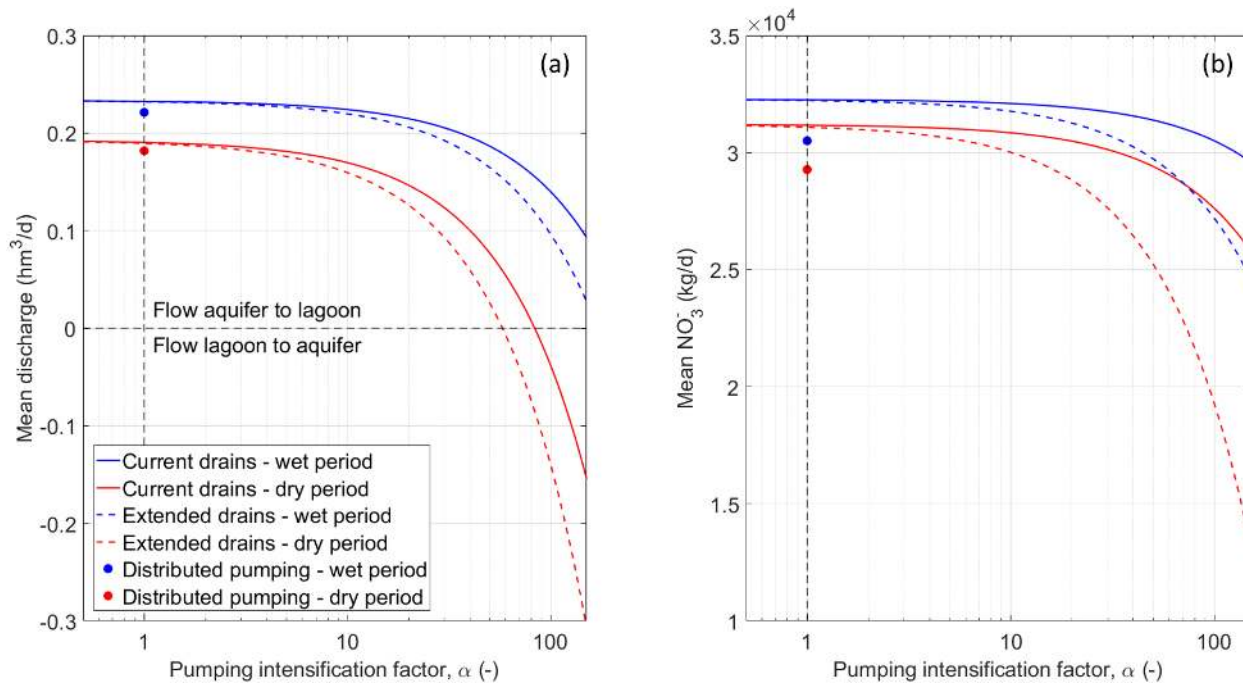
1001   correspond to the three highest recharge values that are out of scale; (b) Daily total discharge of

1002   groundwater (solid black line) and potential nitrate load (dashed grey line) into the lagoon.

1003   Representative average (Apr. 2002–Mar. 2004), wet (Sept. 2008–Aug. 2010) and dry (Sept.

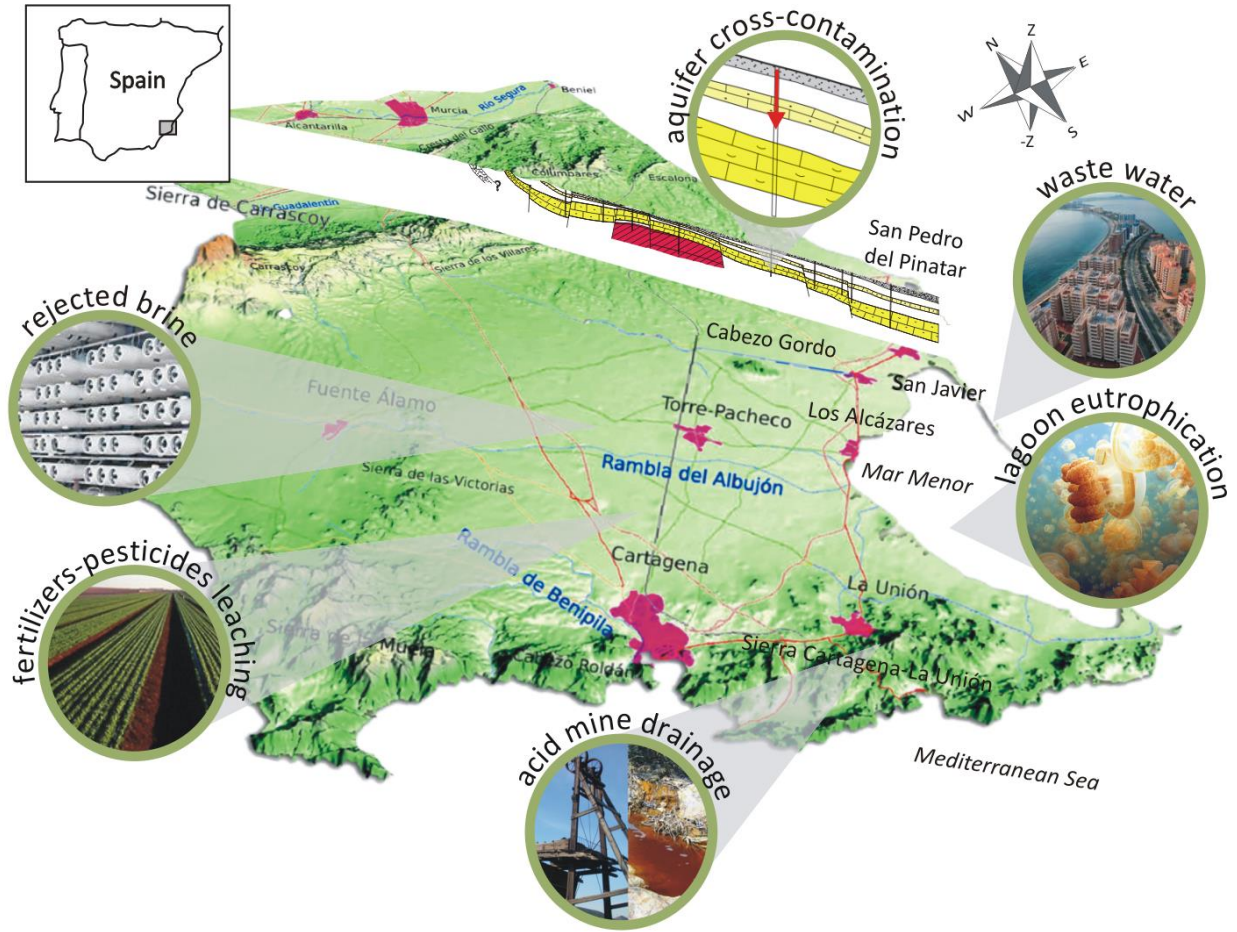1004   2013–Aug. 2015) hydrometeorological periods are shaded.

1005

Figure 11: Potential discharge of groundwater (a) and nitrate (b) into the lagoon under different management scenarios. Discharge is shown as a function of the pumping intensification factor during wet (blue) and dry (red) hydrometeorological periods, for simulation of the localized strategies (scenarios 1 (continuous lines) and 2 (dashed lines), involving pumping from current and current plus extended drains, respectively) and the distributed management strategy (scenario 3).

1022 **Graphical Abstract**

1023